NASA TECHNICAL MEMORANDUM

NASA TM X-71622

NASA TM X-71622

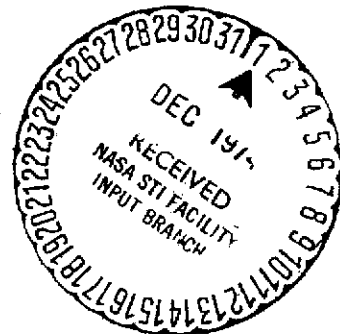# A COMPARISON OF OPTIMUM JP AND LH$_2$ TURBOFAN ENGINES DESIGNED FOR TWO SUBSONIC TRANSPORT MISSIONS

by Kestutis C. Civinskas
U.S. Army Air Mobility R&D Laboratory
Lewis Research Center
Cleveland, Ohio
October 1974

ABSTRACT

Hydrogen fuel is estimated to reduce the gross weight of commercial subsonic transports by 10 to 14 percent, depending upon the design range and payload. Turbofan engine cycles were selected to meet FAR 36 sideline and approach noise goals, without suppression. Three figures-of-merit were calculated: takeoff gross weight, energy consumption, and direct operating cost. The optimum engine cycles were found to be essentially the same for both fuels. No analysis or discussion of the development, operational, or safety problems associated with liquid hydrogen is presented.

E-8145

A COMPARISON OF OPTIMUM JP AND LH$_2$ TURBOFAN ENGINES

DESIGNED FOR TWO SUBSONIC TRANSPORT MISSIONS

by Kestutis C. Civinskas

U.S. Army Air Mobility R&D Laboratory

SUMMARY

This study examines the use of liquid hydrogen fuel in place of conventional JP fuel for two subsonic commercial transports. One is designed to carry 100 passengers a range of 900 naut. miles, and the other, 450 passengers for 3500 naut. miles. The fan pressure and bypass ratio of both were chosen to meet FAR 36 sideline and approach noise goals, without suppression. Fan pressure ratio, bypass ratio, and overall pressure ratio were optimized for a baseline turbine rotor inlet temperature of 2860° R. Three figures-of-merit were considered; takeoff gross weight, energy consumption, and direct operating cost. The technological difficulties of developing and operating cryogenic-fueled aircraft, cost of ground fueling systems, safety, etc. were not considered in the study.

The relatively higher heating value of LH$_2$ reduced the takeoff gross weight by 10% for the shorter-range airplane, and by 14% for the longer-range airplane. Operating empty weight increased by 2 to 4 percent, however. For minimum gross weight and for the baseline $T_4 = 2860°$ R, the optimum cycle for JP was: a FPR of 1.45, OPR of 25, and BPR of about 9.3. For LH$_2$ the optimum cycle was: FPR of 1.5, OPR of 25, and BPR of 8.4. The cycle optimized at about the same values for both missions. One higher value of $T_4 = 3360°$ R was examined with and without cooling bleed to simulate the rejection of turbine cooling heat to the hydrogen fuel and thus avoiding air bleed from the compressor. An additional gross weight improvement of 1 to $2\frac{1}{2}$ percent was observed when there was no bleed. The LH$_2$ airplane had a higher energy con-

sumption: 5 percent higher than the JP-airplane for the short mission, and 10 percent for the long mission. Energy consumption tended to decrease with lower FPR and higher BPR. The optimum cycles for minimum direct operating cost are the same as for minimum gross weight. The design range and payload of the longer-range airplane were perturbed to determine their effect on the relative comparison between JP and LH_2. The advantage of hydrogen fuel over JP improved with increasing range and decreasing payload.

INTRODUCTION

Over the past twenty years, liquid hydrogen (LH_2) has been considered often as a possible alternative to conventional kerosene or JP fuels. Early interest in LH_2 was aimed primarily at improving military aircraft performance. More recently, concern over fossil fuel depletion, rising JP prices, and pollution have spurred interest in LH_2 for commercial aircraft. Its low weight advantage and heat sink capacity have been examined in supersonic and hypersonic applications (refs. 1-5). Its use in subsonic aircraft has also been considered (refs. 6 and 7) with promising results.

The most distinct advantage LH_2 has is a heating value 2.7 times that of JP. A disadvantage, however, is its low density. For a fixed amount of available energy, LH_2 weighs less but requires 4.2 times the volume of JP. The low boiling temperature of LH_2 (-423° F) also requires insulation. These LH_2 containment problems obviously diminish its weight advantage and impose aerodynamic penalties as well.

The objective of the present study was to go beyond a comparison of LH_2 versus JP, and see if the use of hydrogen would result in a significantly different optimum engine. For example, it has been suggested (ref. 8) that by using the cryogenic fuel as a heat sink for turbine cooling purposes, the compressor bleed air in current designs could be eliminated. This, it is suggested further, might lead to a redesign of the engine (higher T_4, pressure ratio) and result in major improvement in SFC

beyond that due to just the higher heating value.

Two subsonic missions were considered in the study. Takeoff gross weight (TOGW), direct operating cost (DOC), and energy consumption were compared for JP and LH_2 versions of the aircraft. Design range and payload were perturbed slightly from one of the missions to observe their effect on TOGW. Engines were selected to meet FAR 36 sideline and approach noise goals without the aid of acoustic suppression. Fan pressure ratios (FPR) and bypass ratios (BPR) were selected to make core jet velocities approach duct jet velocities. An overall pressure ratio of 25 was chosen as a baseline, but two higher values were also considered at one FPR. Turbine rotor inlet temperature (T_4) was initially held fixed at 2860° R. One higher T_4 (3360° R) was also run to examine the benefit of eliminating cooling bleed air from the LH_2 cycle.

ANALYSIS

Mission

Two missions were selected to compare the use of JP and LH_2 subsonically. One was a short-range mission of 900 naut. miles, carrying 100 passengers, baggage, and cargo (payload = 25 000 lb). The other was a long-range mission of 3500 naut. miles and carrying 450 passengers, baggage, and cargo (payload = 177 500). Cruise Mach number was 0.78 in both cases, and cruise altitude was chosen to maximize the Brequet range factor. The flight path is shown in terms of Mach number and altitude in figure 1. ATA domestic reserves, providing for a one-hour hold at cruise altitude and a 200 naut. mile diversion to an alternate airport, were included. It was attempted, as a first cut, to meet FAR 36 sideline and approach noise goals without including suppression.

Airframe

For the short-range mission, the two-engine airplane configuration shown in figure 2 was selected. For a twin-engine airplane of this size, large-diameter, high BPR engines mounted beneath the wings can pose a ground clearance problem. Reference 12 states that under these conditions, there are weight and height advantages to placing the engines in the rear of the fuselage. The JP airplane carries its fuel in the wing and the LH_2 airplane carries it in a full diameter fuselage tank aft of the passenger compartment.

The long-range airplane, shown in figure 3, is a wing-mounted, four-engine configuration based largely on the 747. The JP version of this airplane carries its fuel in the wing. The LH_2 version required extending the upper lobe all the way back to the tail and some rearranging of the galleys. The upper deck lounge was eliminated and the seating was changed from 9 across to 10 across. Figure 4 shows fuselage cross-sections for the long-range LH_2 airplane. For both hydrogen-fueled airplanes, the fuselage length was varied to match the fuel volume to the fuel load that would give the required range. It should be noted that the fuel tank arrangement for the hydrogen airplanes used in this analytical investigation is not necessarily representative of an ultimate arrangement in a practical airplane. The assumed configuration does provide for a representative fuselage volume that would be required with a hydrogen-fueled airplane.

Weights. - The structural, fixed equipment, standard and operational item weight correlations came from a proprietary source. The form of the equations is in some cases similar to those found in reference 13. The wing weight correlation from reference 13 is shown in figure 5. The term $(1 - W_x/W)$ in the wing weight equation is important, for it implies that when the fuel is removed from the wing, the wing becomes heavier. This is a result of the added stiffness that must be built in to make up for the lost bending relief. The LH_2 wing can therefore be heavier than its JP counterpart, even though it is smaller. Some of the geometric and other

parameters assumed for the weight calculation are shown in table II. These were based mainly on characteristics of currently flying aircraft of similar size and configuration. For the short-range aircraft, these were the 737 and DC-9 type aircraft; the model for the long-range aircraft was the 747. Much of the data for these airplanes came from references 14 through 16.

Hydrogen-fuel tankage dimensions and weights. - To obtain better surface/volume ratio for insulation, and to obtain more easily the large volume required by LH_2, the hydrogen fuel tanks were placed entirely within the fuselage. Tank pressurization to eliminate boiloff during climb can also be more easily implemented with cylindrical fuselage tanks, rather than with irregular-shaped wing tanks. To calculate the fuel tank volume and insulation requirements, a first-order estimate of the expected boiloff was performed. The boiloff due to heat flow through the tank walls depends on the amount and type of insulation applied. The heat flow per unit area into the fuel can be expressed as

$$Q_{in} = \frac{K \, \Delta T \, \Delta t}{th}$$

where

K   thermal conductivity of insulation, Btu-in./ft^2/hr/^oR

ΔT temperature difference across insulation, ^oR

Δt time interval, hr

th   thickness of insulation, in.

The weight of boiloff fuel per unit area due to heat flow into the tank is then just equal to

$$(W_f)_{b.o.} = \frac{Q_{in}}{Q_v}$$

where Q_v is the heat of vaporization of LH_2, Btu/lb. The weight of insulation per unit area is

$$W_{in.} = \frac{\rho_{in.} \, th}{12}$$

where $\rho_{in.}$ is the density of insulation, lb/ft^2. There is a tradeoff to be made between heat boiloff fuel and insulation weight. Writing the sum of these, differentiating, and setting to zero, the thickness for minimum weight turns out to be

$$th_{min. \, wt.} = \sqrt{\frac{12K \, \Delta T \, \Delta t}{\rho_{in.} \, (Q_v)}}$$

Insulation was assumed to be polyurethane foam, properties of which are shown in table III. The insulation thickness for the short- and long-range missions was calculated to be about 2.75 and 5.0 in., respectively. Heat boiloff amounted to approximately 5 percent of total fuel and was accounted for in the flight calculations by degrading SFC. The boiloff could, at the cost of some added complexity, be burned in the engines, or used for cooling, but neither option was assumed in the study. The tanks were assumed designed for a high enough ΔP that there was no pressure boiloff with increasing altitude. For the cruise altitudes of this study (approx. 30 000 ft), the tank design of reference 6 was found to be adequate for this assumption. The safety factor would be somewhat lower than for the design application of reference 6, however. The tank weights were based on a "smear" thickness of 0.1 in. (this is an effective thickness, including stiffeners and baffles). The actual skin thickness is only about one-half the "smear" thickness. This approach results in about twice the tank weight compared to the equation used in reference 2. The short-range-airplane tank was 10 feet in diameter. The long-range had 8 and 10 foot diameter tanks located as shown in the cross-sectional

view in figure 4. Allowance of 6 to 9 inches was made around the tanks to allow for the insulation, attachments, etc. To keep the required fuselage extension for the long-range airplane down to a minimum, the upper lounge was eliminated, galleys were rearranged (same total volume), and the seating arrangement was changed from 9 to 10 across.

JP airplanes typically have some excess fuel capacity at the max. payload/max. TOGW condition. This provides the option of adding fuel at the expense of reduced payload to permit some longer range missions. Because of the volume difficulties associated with LH_2, the hydrogen airplane was designed with no excess fuel capacity. This is a slight disadvantage for the LH_2 airplane, as its flexibility for varied range operations is not as great.

Aerodynamics. - The aerodynamics of the airplanes in this study were based on drag polars obtained from industry for several current subsonic airplanes. The cruise L/D for the short-range airplane was about 13. For the long-range airplane, it was about 20. It was assumed that the drag polars could be described by the parabolic equation

$$C_D = C_{D_{min}} + \left[\frac{C_{D_i}}{\left(C_L - C_{L_o}\right)^2} \right] \left(C_L - C_{L_o}\right)^2 \tag{1}$$

where

C_L lift coefficient

C_D drag coefficient

$C_{D_{min}}$ minimum drag coefficient

C_{D_i} induced drag coefficient

C_{L_o} lift coefficient where $C_{D_{min}}$ occurs

Schedules of $C_{D_{min}}$, $\left[C_{D_i} \middle/ \left(C_L - C_{L_o}\right)^2\right]$, and C_{L_o} with Mach number were then determined. The reference set of these coefficients is shown plotted against Mach number in figures 6 and 7. Since the relative areas of wings, fuselage, etc. will change by going from JP to LH_2, the drag polars represented by these coefficients must be adjusted to account for these area changes. A component drag build-up is required for this adjustment. The airframe was taken to be made up of wing, body, horizontal tail, vertical tail, and engine nacelles. The minimum drag can be written as the sum of friction and pressure drags

$$C_{D_{min}} S_w q = C_{D_f} S_w q + C_{D_p} S_w q \tag{2}$$

where

S_w wing planform area, ft^2

q dynamic pressure, lb/ft^2

C_{D_f} total friction drag coefficient

C_{D_p} pressure drag coefficient

Writing the friction drag in terms of the components, and dividing through by $S_w q$, an expression for $C_{D_{min}}$ results:

$$C_{D_{min}} = 2\left(C_{fw} + C_{fvt} \frac{S_{vt}}{S_w} + C_{fht} \frac{S_{ht}}{S_w}\right) + C_{fn} N \frac{S_n}{S_w} + C_{fb} \frac{S_b}{S_w} + C_{D_p} \tag{3}$$

where

C_f component friction coefficient

S area, ft^2

N number of engines

Subscripts

w   wing

vt   vertical tail

ht   horizontal tail

n   nacelle

b   body

The skin friction coefficients can be calculated from the Prandtl-Schlichting equation

$$C_f = 0.455(\log Re)^{-2.58} \tag{4}$$

where Re is Reynold's number for the component. This equation gives the skin friction coefficient for incompressible turbulent flow over one surface of a flat plate. To account for compressibility effects, these coefficients were then corrected by a factor which was a function of Mach number and altitude. Calculating the component friction coefficients and using typical component areas for the reference airplanes (short- and long-range), equation (3) was solved to obtain a reference C_{D_p} versus Mach number schedule. This reference C_{D_p} and the C_{L_o}, $C_{D_i} / \left(C_L - C_{L_o}\right)^2$ were assumed not to change with variation in relative component dimensions. The $C_{D_{min}}$, however, was allowed to vary with area ratios according to equation (3). The skin friction coefficients change also because of characteristic length changes in the Reynold's number term of equation (4).

Engines

The engines used in the study were separate-flow, two-spool turbofans. Current engine weight and performance technology were assumed. The engines were all designed at sea level static, and design turbine-

rotor-inlet temperature was initially held fixed at 2860° R. Overall pressure ratio, fan pressure ratio, and bypass ratio were varied. For fan and overall pressure ratio combinations requiring a compressor pressure ratio greater than 16, booster stages were added to the fan spool. At a fan pressure ratio of 1.6, three overall pressure ratios were examined: 25, 30, and 35. At an overall pressure ratio of 25, three fan pressure ratios were considered: 1.5, 1.6, and 1.7. One higher T_4 (3360° R) was considered at an OPR of 30 and FPR of 1.6.

Design point for all engines was at sea level static, standard day. Design and off-design performance was calculated using the GENENG computer program of reference 17. To get the specific fuel consumption of the LH_2 engines, SFC was taken to vary inversely with heating value. This approach has been shown in reference 18 to involve negligible error. A summary of component characteristics at sea level and cruise conditions is given in table IV for a representative engine used in this study. The data are for the short-range JP case, for which the sea level static airflow was 574 lb/sec per engine. The amount of T_4 cutback at cruise is dependent upon the gross weight, the L/D, and the engine size as determined by the sea level static thrust to weight ratio. The minimum T_4 cutback was 100° R. A range of bypass ratios was examined for each FPR that cut core jet noise down to about the level of duct jet noise, since that source is established mainly by the fan pressure ratio. Fan and compressor design efficiencies were varied with design pressure ratio according to the schedules shown in figures 8 and 9. The fan schedule is the result of simply plotting some existing and study fans, and noting a definite trend. When this approach was tried with compressors, there was so much scatter that no trend could be observed, and a different method was used. The relationship between pressure ratio, polytropic efficiency, and adiabatic efficiency was plotted and a value of 0.89 polytropic efficiency was picked as representative of current state-of-the-art. The resulting schedule is indicated on figure 9. Turbine cooling bleed requirements were estimated as functions of turbine stages, turbine inlet temperature, etc., according to the method outlined in ref-

erence 19. Maximum metal temperatures assumed for the rotors and stators were 2210° and 2310° R, respectively. The number of LP turbine stages was approximated roughly as a function of bypass ratio. The bare engine weight was estimated using the correlations in reference 20. A 1.1 installation factor was applied to account for inlet, nozzles, and other installation items. Physical differences between a JP and LH_2 engine are minor, as indicated in reference 21. The LH_2 engine has a somewhat more complicated fuel system, but it also has the possibility of a shorter combustor. The magnitude of these differences was taken to be small, so that the engine weights and dimensions were assumed to be independent of fuel type, as was done in reference 18.

Precise calculation of the required thrust for an airplane involves a complicated examination of takeoff and landing characteristics with and without engine failures for selected field lengths, together with attention to climb and cruise performance. To simplify this procedure, a purely empirical approach was adopted in which a correlation was sought for the takeoff thrust/weight ratio of existing airplanes (fig. 10). The lower curve shows the trend for low BPR engines such as the JT3D, -8D class of engines. The upper curve shows the JT9D, CF6 class engines. The figure reflects the effect that number of engines has on the engine-out requirements of the airplane. With fewer engines, the loss of an engine represents a larger loss of thrust percentage-wise, and so the maximum installed thrust per engine has to be greater. The bypass variation is a result of the greater thrust lapse that the higher BPR engines experience with altitude.

Extrapolating the higher BPR curve out to 2 engines, a takeoff thrust/weight of 0.33 was chosen for the short-range airplane. A takeoff thrust/weight of 0.25 was picked for the long-range, 4-engine airplane. This choice resulted in most of the airplanes having enough thrust to reach optimum cruise altitude. The few that did not were within several percent of the maximum Brequet factor anyway.

Noise. - Noise was calculated both at sideline and approach. The standard SAE method (ref. 22) was used to calculate jet noise of the hot stream. For the duct or cold stream, a modification to the SAE method was made to get better agreement with published data such as in reference 23. Noise measurement experience with airplanes flying under actual conditions has produced the following approximate corrections to convert PNdB to EPNdB: for sideline noise, EPNdB = PNdB; for approach, EPNdB = PNdB - 5dB. Sideline noise is calculated at lift-off (approx. Mach 0.2) along a 0.25 n. mi. sideline for the 2-engine airplane, and along a 0.35 n. mi. sideline for the 4-engine airplane. For sideline noise, the engines operate at maximum thrust ($T_4 = 2860^O$ R). On approach, noise is calculated 1 n. mi. from the end of the runway and with a 3° glide slope. Under these conditions, the aircraft is at an altitude of 368 ft at that point. The engine thrust was cut back to about 33 percent for the approach noise calculations. Fan machinery noise was estimated from an empirical equation supplied by Dr. F. Montegani of the LeRC V/STOL and Noise Division. This formula is shown in graphical form in figure 11 and is based largely on empirical data such as in reference 24. The curve shown in the figure was adjusted for thrust level, distance, and air attenuation for each engine and airplane. No suppression was assumed throughout the study, but the fan noise is based on designs (tip speeds, rotor-stator spacings, etc.) that yield low noise.

Direct operating cost. - A better figure of merit for a commercial transport than gross weight, is an economic one - such as direct operating cost (DOC). DOC was calculated for each engine assuming an airframe cost of $75/lb and an engine cost of $110/lb. The standard ATA formulas of reference 25 were used. The DOC is a function of TOGW and fuel price, among other things. The relative standings of the two airplanes will be greatly affected by their relative fuel cost. Two price levels of JP were assumed, 20 and 30 cents per gallon. Today's fuel costs depend on many factors and vary according to airline and location. Thirty cents per gallon is higher than what domestics are paying for

fuel, but lower than what the international flights are paying.

Costs of LH_2 are highly speculative, ranging in on reference (26) from 11.7 to 43.5 cents per pound, depending upon the method used to produce it. One of the values used here, 10 cents per pound, was taken from reference 27 and is based on steam-reformed natural gas. One higher value, 15 cents per pound, was also run. Expressed in energy units, the two values of fuel prices were $1.67 and $2.00 per million Btu for JP; and $2.00 and $3.00 per million Btu for LH_2. A break-even curve was derived to show which DOC (JP or LH_2) would be higher for any other values of fuel cost.

RESULTS AND DISCUSSION

A weight breakdown of representative JP and LH_2 airplanes is shown in figure 12 for both missions. The hydrogen airplane achieved about a 10 percent reduction in gross weight on the short mission, and about 14 percent over the longer-range mission. This improvement in gross weight is less than that shown in some other LH_2 studies (e.g., roughly half of that shown in ref. 8). While tail and landing gear weights decreased for the LH_2 airplane, the body weight increased. The wing weight goes up for the long-range airplane, and down for the short-range airplane (tables V and VI). The wing loading for each airplane was kept constant at the value shown in table II. In the case of the long-range airplane, the JP fuel fraction is large enough that when we go to LH_2 and put the fuel in the fuselage, the bending relief factor makes the wing design heavier, even though it will be smaller in area. The effect of this factor on gross weight and operating empty weight was examined by running one LH_2 case with a JP-type wing. That is, a wing that was designed to carry an amount of JP fuel appropriate for that mission. This dummy fuel weight was not included in the gross weight of the hydrogen airplane and the LH_2 fuel was still assumed to be in the fuselage. Under these conditions, the improvement in gross weight from JP to LH_2 rose from 14 to 22 percent and caused

the LH_2 operating empty weight to be 8 percent lower than for JP. This result would indicate that placing the LH_2 in or on the wing might be a preferable configuration from the weight standpoint, although it would impose a greater aerodynamic penalty (e.g., ref. 8).

The takeoff gross weight variation with fan pressure ratio and bypass ratio is shown in figures 13 and 14 for the two aircraft. The gross weights show little sensitivity to fan pressure ratio, although there is a trend more readily seen in the short-range case to go to higher FPR. The approach and sideline noise are indicated in the figures above and below the curves, respectively. FAR 36 specifies a sideline noise goal of 95 EPNdB and an approach noise goal of 103 EPNdB for a 100 000 lb gross weight aircraft. By crossplotting and extrapolating slightly beyond the range of FPR's examined, the cycle that minimizes TOGW and meets this noise constraint for $T_4 = 2860^O$ R and OPR = 25 was: FPR = 1.45, BPR = 9.5 for the JP airplane, and FPR = 1.5, BPR = 8.4 for the LH_2 airplane. These numbers are for the short-range airplane. For the long-range airplane, FAR 36 specifies a noise goal of 108 EPNdB both for approach and sideline. The best cycles in this case were: FPR = 1.46, BPR = 9.2 for JP and FPR = 1.5, BPR = 8.4 for LH_2. Because of lower gross weight, and therefore lower engine airflow and noise, the LH_2 engines optimize at slightly higher FPR and lower BPR, which is the direction that they would optimize to without noise constraints. The best cycles for the short- and long-range missions, are, for all practical purposes, the same.

Figures 15 and 16 show the sensitivity of the gross weights to overall pressure ratio. The OPR was increased from the baseline value of 25 to 30 and 35. It can be deduced from the figures that the percentage improvement in gross weight between LH_2 and JP stays unchanged as OPR varies, and, in fact, there is no advantage in going to higher overall pressure ratios for a T_4 of 2860° R - either with JP or LH_2.

One case of higher T_4 was run to examine the performance advantage of eliminating compressor bleed by somehow employing the LH_2

heat sink capacity. The engine weights were not penalized for this increase in T_4. Figure 17 shows the results for a FPR of 1.6, OPR of 30, and T_4 of 3360° R. The higher T_4 improves the thrust/weight of the engine by about 11 percent. However, at this T_4, turbine cooling requirements using uncooled compressor bleed air for full-film cooling go from about 4 to 12 percent. (This, and all subsequent reference to cooling bleed air, should be taken to mean chargeable bleed.) The SFC losses due to this additional bleed cancel the benefit to be expected from the lower engine weight, and the TOGW is not reduced. However, it may be possible to reject heat to the fuel and substantially reduce or possibly even eliminate compressor bleed for turbine cooling. As an extreme case, the cooling air was assumed to be eliminated altogether with no other penalties imposed. The consequent reduction in TOGW was only about 1 to $2\frac{1}{2}$ percent. As far as noise is concerned at this higher T_4, the 12 percent bleed cases have about the same noise levels as $T_4 = 2860^O$ R because the BPR was increased. The sideline noise for the zero bleed case, though, is about 10 dB higher and would require even higher BPR. Since the TOGW curves become relatively flat with increasing BPR, however, the conclusion drawn regarding the benefit of higher T_4 would be unchanged.

The next two figures, 18 and 19, compare the JP and LH_2 airplanes in terms of energy consumption. Overall, the energy consumption drops for the larger airplane, reflecting its better cruise L/D. Energy consumption is 5 to 10 percent higher for the hydrogen airplane, though, indicating that the decreases in its gross weight did not sufficiently offset aerodynamic penalties. If optimized for low energy consumption, the FPR tends toward lower values, rather than higher, as when optimized for gross weight. As FPR drops, BPR would increase to keep core jet velocity down.

The DOC results are shown in figures 20 and 21. The variation of DOC with FPR over the range 1.5 to 1.7 is practically negligible. Since the minimum's of these curves occur at the same BPR's as the gross weight curves, the same optimum cycles based on gross weight and

meeting FAR 36 noise constraints would serve equally well for minimizing DOC. Direct operating cost depends, of course, greatly on the fuel prices assumed. The sensitivity of DOC to fuel price can be seen parametrically in figures 20 and 21. The relative DOC between JP and LH_2 will be entirely dependent on the fuel prices assumed for both. Figure 22, therefore, shows the DOC break-even prices of JP and LH_2 fuel for one of the study airplanes.

Figure 23 shows the sensitivity of the LH_2 gross weight improvement with variations of design range and payload. For the 450-passenger airplane, the range was decreased to 3000 and 2500 n. mi. Then, for a 3000 n. mi. range, the number of passengers was decreased to 400 and 350. The benefit of switching to LH_2 is seen to increase with range and decrease with number of passengers. Increasing range increases the fuel fraction, and the greater the fuel fraction, the greater is the effect of switching to an alternate fuel. Increasing the payload for a fixed range has the opposite effect since more of the aircraft gross weight is now fixed, and the fuel fraction decreases slightly.

CONCLUDING REMARKS

The results of this study indicate that hydrogen fuel could decrease takeoff gross weight of commercial subsonic transports by 10 to 14 percent, depending upon the design range and payload. The gross weight advantage of going to LH_2 increases with increasing range and decreasing payload. Designed to meet FAR 36 sideline and approach noise goals, the optimum engine cycles are the same for long- and short-range missions. Designed for the same payload and range, and using the same cycle, the LH_2 airplane would achieve slightly lower noise goals because of its smaller size. The LH_2 engines optimize at slightly lower BPR and higher FPR. The optimum engine cycles based on minimum takeoff gross weight are the same as those based on minimum DOC. Minimizing energy consumption tends toward lower FPR and higher BPR. The advantage of eliminating compressor bleed air for turbine cooling by

rejecting the heat to hydrogen fuel gives the LH_2 airplane only an additional 1 to $2\frac{1}{2}$ percent improvement in gross weight. No further engine benefit could be identified for hydrogen other than that due to the heating value advantage.

The above relative comparisons between JP and LH_2 could significantly change when considerations which were not in this study are included. Safety, availability, handling, future price, and scarcity of JP fuel would all have to be weighed. This preliminary study does suggest, however, that the engine cycles for a LH_2-fueled subsonic transport will be basically the same as the conventional turbofans used for JP aircraft.

REFERENCES

1. Escher, W. J. D.; and Brewer, G. D.: Hydrogen: Make - Sense Fuel for an American Supersonic Transport. AIAA Paper 74-163, presented at AIAA 12th Aerospace Sciences meeting, Washington, D. C., Jan. 30-Feb. 1, 1974.

2. Whitlow, John B., Jr.; Weber, Richard J.; and Civinskas, Kestutis C.: Preliminary Appraisal of Hydrogen and Methane Fuel in a Mach 2.7 Supersonic Transport. NASA TM X-68222, 1973.

3. Weber, Richard J.: Propulsion for Hypersonic Transport Aircraft. Proceedings of the Fourth Congress of the International Council of the Aeronautical Sciences. R. R. Dexter, ed. Spartan Books, Inc., 1965, pp. 977-999.

4. Witcofski, Robert D.: Hydrogen Fueled Hypersonic Transports, presented at the American Chemical Society Symposium on Non-Fossil Chemical Fuels, Boston, Mass., April 9-14, 1972.

5. Helenbrook, R. G.; McConarty, W. A.; and Anthony, F. M.: Evaluation of Active Cooling Systems for a Mach 6 Hypersonic Transport Airframe. Bell Aerosystems Co. report No. 7305-902001, Sept. 1969.

6. Advanced Transport Technology Engineering Staff: A Fuel Conservation Study for Transport Aircraft Utilizing Advanced Technology and Hydrogen Fuel. LTV Aerospace Corp., NASA CR-112204, Nov., 1972.

7. Strack, W. C.: Preliminary Performance Appraisal of Navy V/STOL Transport and Search - Type Airplanes Using Hydrogen Fuel. NASA TM X-71550, May, 1974.

8. Brewer, G. Daniel: The Case for Hydrogen - Fueled Transport Aircraft. AIAA, May, 1974.

9. Eisenberg, Joseph D.: High-Energy Fuels for Supersonic Transport Reserves. NASA TN D-3987, 1967.

10. Perry, John H., ed.: Chemical Engineer's Handbook. 4th ed., McGraw-Hill Book Co., Inc., 1963.

11. Anon.: Data Book and Buyer's Guide/73. Cryogenic and Industrial Gases, May/June, 1973.

12. Williams, P. R. G.; and Stewart, D. J.: An Aircraft Designer's Review of Some Airframe and Engine Integration Concepts. Paper presented at 1st International Symposium on Air Breathing Engines. (Marseille), June, 1972.

13. Warnock, W. E.: Special Considerations in the Weight Estimation of Features Unique to VTOL Airplanes.

14. Anon.: Jane's All the World's Aircraft 1972-73, McGraw-Hill Book Co., 1972.

15. Harrison, Neil: Boeing 737 - A Short-Hauler Engineered for Efficiency. Flight International, Feb. 3, 1966, pp. 181-188.

16. Harrison, Neil: Boeing 747. Flight International, December 12, 1968, pp. 979-997.

17. Fishbach, Lawrence H.; and Koeing, Robert W.: GENENG II - A Program for Calculating Design and Off-Design Performance of Two and Three Spool Turbofans With as Many as Three Nozzles. NASA TN D-6553, 1972.

18. Sabatella, J.; Johnson, J.; and Aronstamm, G.: Advanced Supersonic Propulsion System Technology Study/Task IV Report, H_2 Fuel Engines (1980 Technology). PWA-TM-4787, Pratt & Whitney Aircraft, 1973.

19. Kraft, Gerald A.; and Whitlow, John B., Jr.: Optimization of Engines for a Commercial Mach 0.98 Transport Using Advanced Turbine Cooling Methods. NASA TM X-68031, March, 1972.

20. Gerend, Robert P.; and Roundhill, John P.: Correlation of Gas Turbine Engine Weights and Dimensions. Paper 70-699, AIAA, June, 1970.

21. Anon.: Alternative Aircraft Fuels and Application - Feasibility of Hydrogen-Fueled Long-Range Transports. Report ADR 74-66-1, Douglas Aircraft Co., 1974.

22. Anon.: Jet Noise Prediction. Aerospace Information Rep. 876, SAE, July 10, 1965.

23. Kramer, James J.; Chestnutt, David; Kresja, Eugene A.; Lucas, James G.; and Rice, Edward J.: Noise Reduction. Aircraft Propulsion. NASA SP-259, 1971, pp. 169-209.

24. Feiler, Charles E.; and Conrad, E. William: Noise from Turbomachinery. NASA TM X-68253, 1973.

25. Anon.: Standard Method of Estimating Comparative Direct Operating Costs of Turbine Powered Transport Airplanes. Air Transport Association of America, Dec., 1967.

26. Johnson, John E.: The Economics of Liquid Hydrogen Supply for Air Transportation. Paper presented at the Cryogenic Engineering Conference (Atlanta, Ga.), August, 1973.

27. Small, W. J.; Fetterman, D. E.; and Bouner, T. F., Jr.: Potential of Hydrogen Fuel for Future Air Transportation Systems. ASME paper No. 73-ICT-104, 1973.

TABLE I.- FUEL PROPERTIES

	JP	LH$_2$
HEATING VALUE, BTU/LB.	18600[a.]	49900[b.]
DENSITY, LB/FT^3	50	4.4
BOILING POINT, °F	350	-423
SPECIFIC HEAT, C_p, BTU/LB/°R	0.47	1.75
HEAT OF VAPORIZATION, Q_v, BTU/LB.	—	191.9
HEAT SINK CAPACITY, BTU/LB.	300 @700°F	4902 @1000°F
REFERENCES	9	10 AND 11

a. AT 537°R
b. AT 37°R

TABLE II. — AIRPLANE CHARACTERISTICS

	100 PASS. 900 N.MI.	450 PASS. 3500 N.MI.
FLIGHT CREW	2	3
WING LOADING, LB/FT^2	100	130
WING ASPECT RATIO, AR	8.0	7.0
WING SWEEPBACK @ ¼ CHORD, DEG.	25	37.5
FUSELAGE WIDTH, FT	12.5	21.0
LANDING WT./TOGW, %	90	80
ULTIMATE LOAD FACTOR, N	3.75	3.75
TAKEOFF THRUST/WEIGHT	0.33	0.25
CRUISE L/D (TYPICAL) { JP	12.9	19.6
CRUISE L/D (TYPICAL) { LH$_2$	11.9	17.6

TABLE III — INSULATION PROPERTIES

	POLYURETHANE
THERMAL CONDUCTIVITY, K, BTU-IN/FT^2/HR/°R	0.20
DENSITY, LB/FT^3	2.0

TABLE IV. CYCLE PARAMETERS OF A REPRESENTATIVE ENGINE

	DESIGN @ SEA LEVEL STATIC	CRUISE @ MACH 0.78 33,000'
INLET PRESSURE RECOVERY	0.98	0.98
FAN PRESSURE RATIO	1.6	1.66
COMPRESSOR PRESSURE RATIO	15.6	16.1
BYPASS RATIO	7.3	7.4
FAN ADIABATIC EFFICIENCY	0.864	0.861
COMPRESSOR ADIABATIC EFFICIENCY	0.844	0.839
TURBINE ROTOR INLET TEMP., $^\circ R$	2860	2560
COMBUSTOR $\Delta P/P_{IN}$	0.02	0.02
COMBUSTOR EFFICIENCY	0.99	0.99
FAN DUCT $\Delta P/P_{IN}$	0.02	0.02
COOLING BLEED, % COREFLOW	3.8	3.8
% TO HP TURBINE	94	94
% TO LP TURBINE	6	6
HP TURBINE ADIABATIC EFFICIENCY	0.90	0.90
LP TURBINE ADIABATIC EFFICIENCY	0.89	0.89
CORE NOZZLE $\Delta P/P_{IN}$	0.02	0.02
DUCT NOZZLE VELOCITY COEFFICIENT	0.98	0.98
CORE NOZZLE VELOCITY COEFFICIENT	0.98	0.98

TABLE V. WEIGHT BREAKDOWN FOR 100-PASS. AIRPLANE. (FPR=1.5, OPR=25, BPR=8.8)

	JP		LH$_2$	
	WEIGHT, LB	%GROSS WT.	WEIGHT, LB	%GROSS WT.
WING	10124	10.01	9906	10.90
TAIL	2477	2.45	2181	2.40
BODY	12799	12.65	13569	14.93
LAND. GEAR	3933	3.89	3710	4.08
OTHER STRUCT.	1692	1.67	1326	1.46
TOTAL STRUCTURE	31025	30.68	30691	33.76
PROPULSION *	7626	7.54	8546	9.40
FIXED EQUIPMENT	16249	16.07	16223	17.85
OPERATIONAL ITEMS	3735	3.69	3554	3.91
OPERATING EMPTY WT.	58635	57.97	59013	64.92
FUEL	17505	17.31	7117	7.83
PAYLOAD	25000	24.72	25000	27.50
TAKEOFF GROSS WT.	101140	100.00	90899	100.00

* INCLUDES INSULATED FUEL TANKS FOR HYDROGEN AIRPLANE.

TABLE VI. WEIGHT BREAKDOWN FOR 450-PASS. AIRPLANE. (FPR=1.5, OPR=25, BPR=8.8)

	JP		LH_2	
	WEIGHT, LB	%GROSS WT.	WEIGHT, LB	%GROSS WT.
WING	92610	12.65	97161	15.51
TAIL	13034	1.78	11276	1.80
BODY	73828	10.09	79904	12.76
LAND.GEAR	30516	4.17	28717	4.58
OTHER STRUCT.	11666	1.59	9812	1.57
TOTAL STRUCTURE	221654	30.29	226870	36.22
PROPULSION *	44509	6.08	54568	8.71
FIXED EQUIPMENT	68060	9.30	71009	11.34
OPERATIONAL ITEMS	15599	2.13	15305	2.44
OPERATING EMPTY WT.	349822	47.80	367752	58.71
FUEL	204541	27.95	81082	12.95
PAYLOAD	177500	24.25	177500	28.34
TAKEOFF GROSS WT.	731863	100.00	626334	100.00

* INCLUDES INSULATED FUEL TANKS FOR HYDROGEN AIRPLANE.
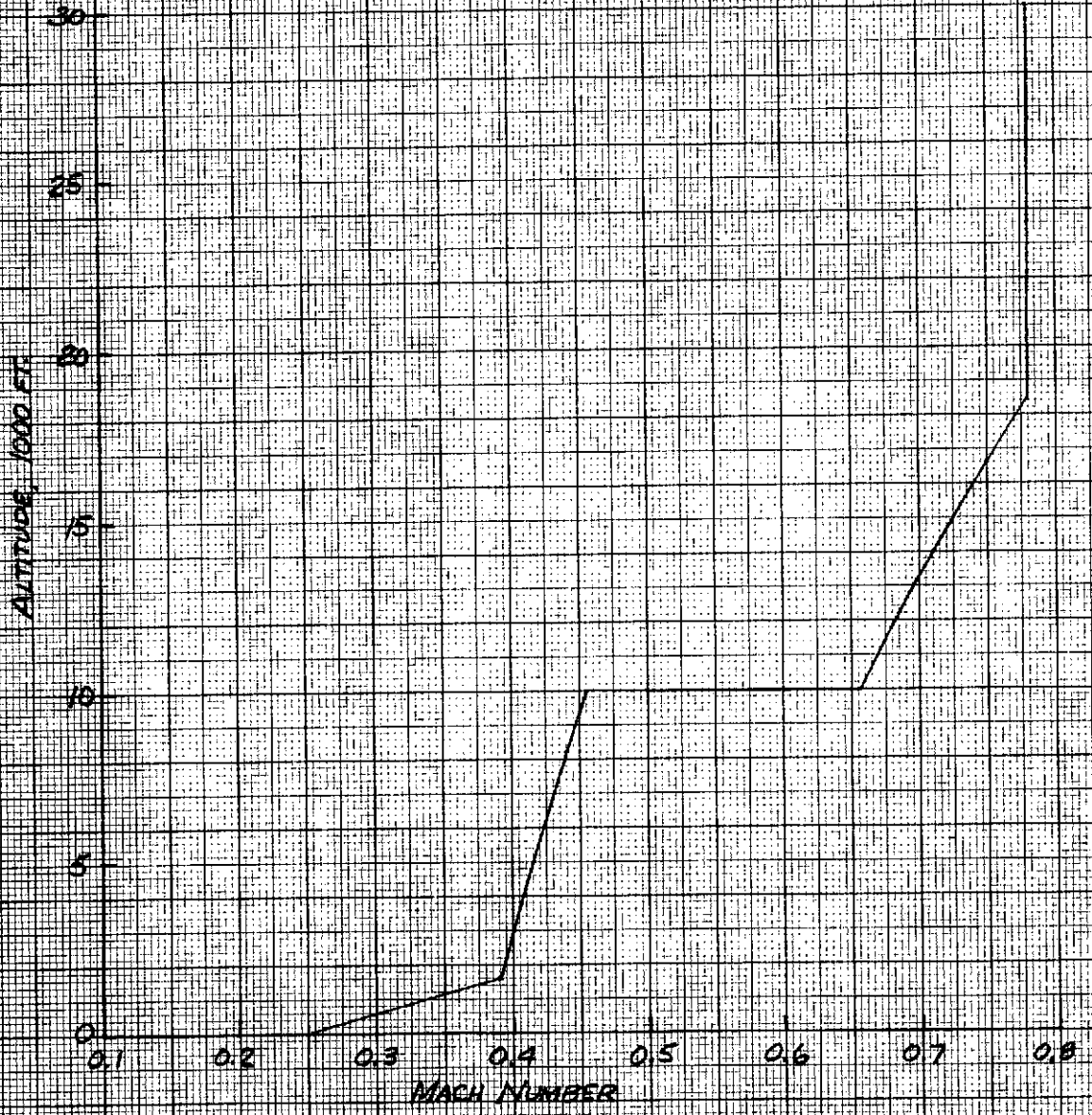
FIGURE 1. — MACH NO.-ALTITUDE FLIGHT PATH

JP
FUEL

COCKPIT

PASS.

CARGO | WING BOX | CARGO

a) JP-FUELED CONFIGURATION

COCKPIT

PASS.

CARGO | WING BOX | LH₂
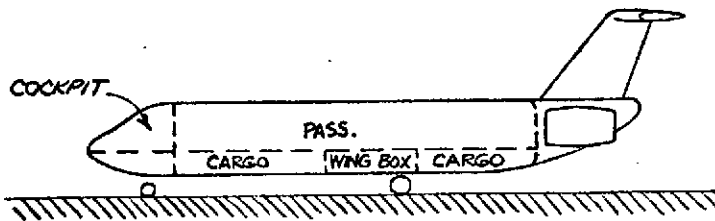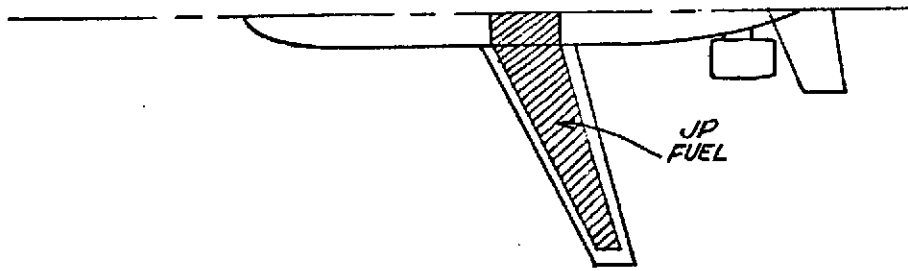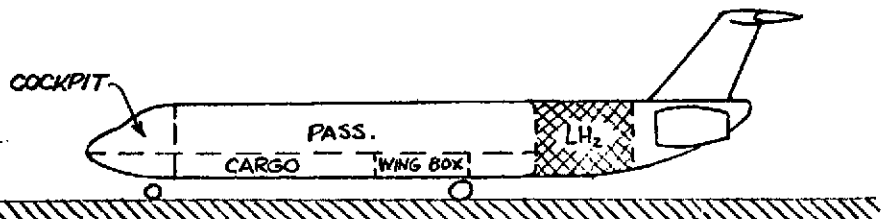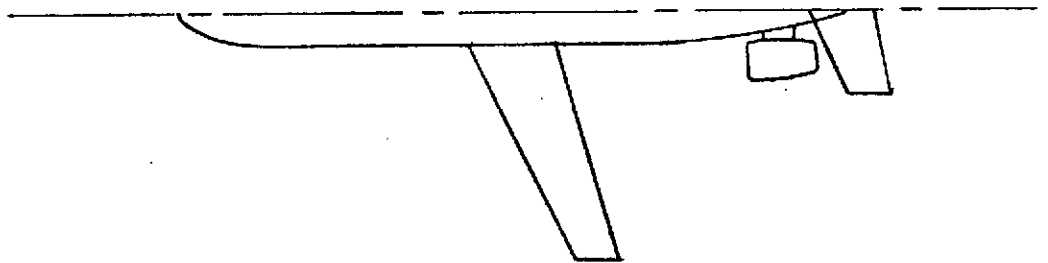
b) LH₂-FUELED CONFIGURATION

FIGURE 2. — 100-PASSENGER, 900 N.MI. AIRPLANE.

LOUNGE
COCKPIT
GALLEYS

PASS.

NOSE WHEEL
COMPARTMENT

CARGO   WING BOX   CARGO

JP
FUEL

a) JP-FUELED CONFIGURATION

GALLEY
COCKPIT

NOSE
WHEEL
COMPARTMENT

PASS.

PASS.

LH₂

CARGO   LH₂   WING BOX

A

B

b) LH₂-FUELED CONFIGURATION
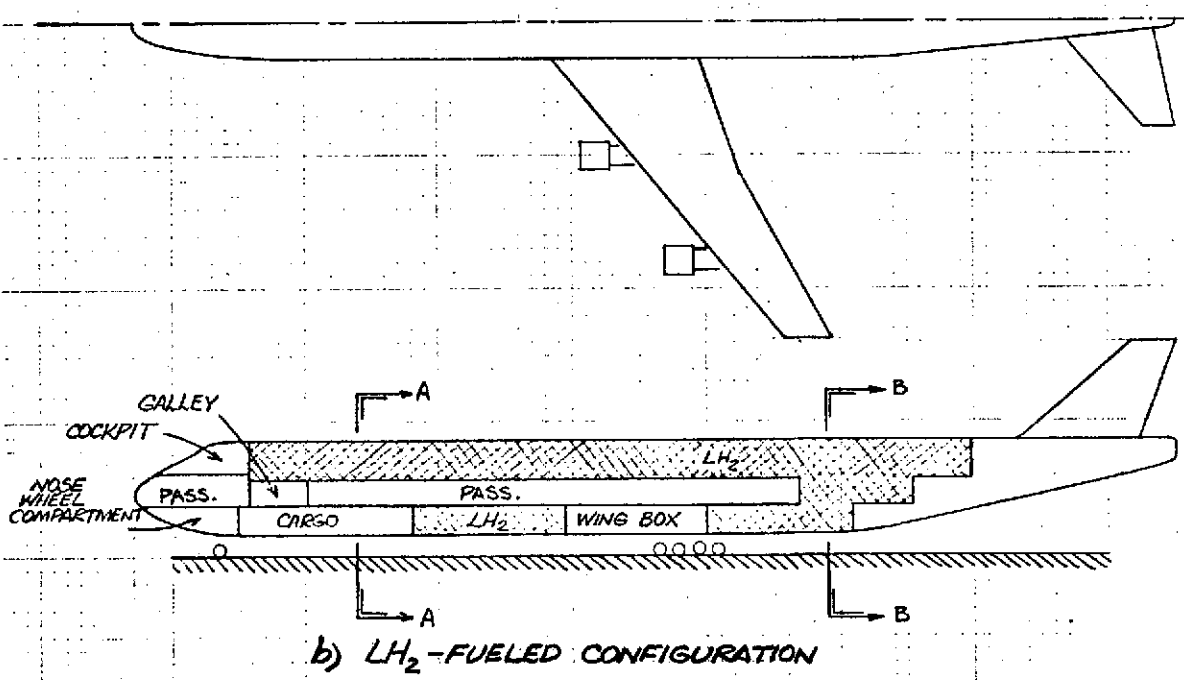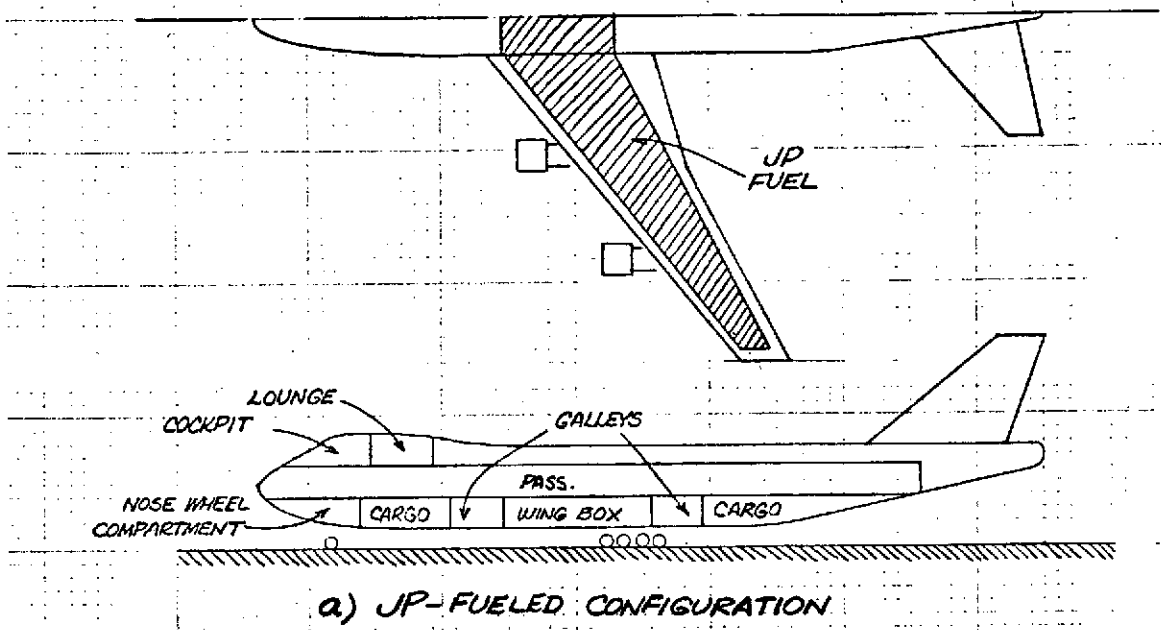
FIGURE 3. — 450 PASSENGER, 3500 N.MI. AIRPLANE.

SECTION A-A

SECTION B-B

10' DIA. TANK

8' DIA. TANKS

LH$_2$

LH$_2$

LH$_2$

LH$_2$

LH$_2$

CARGO

27'

21'
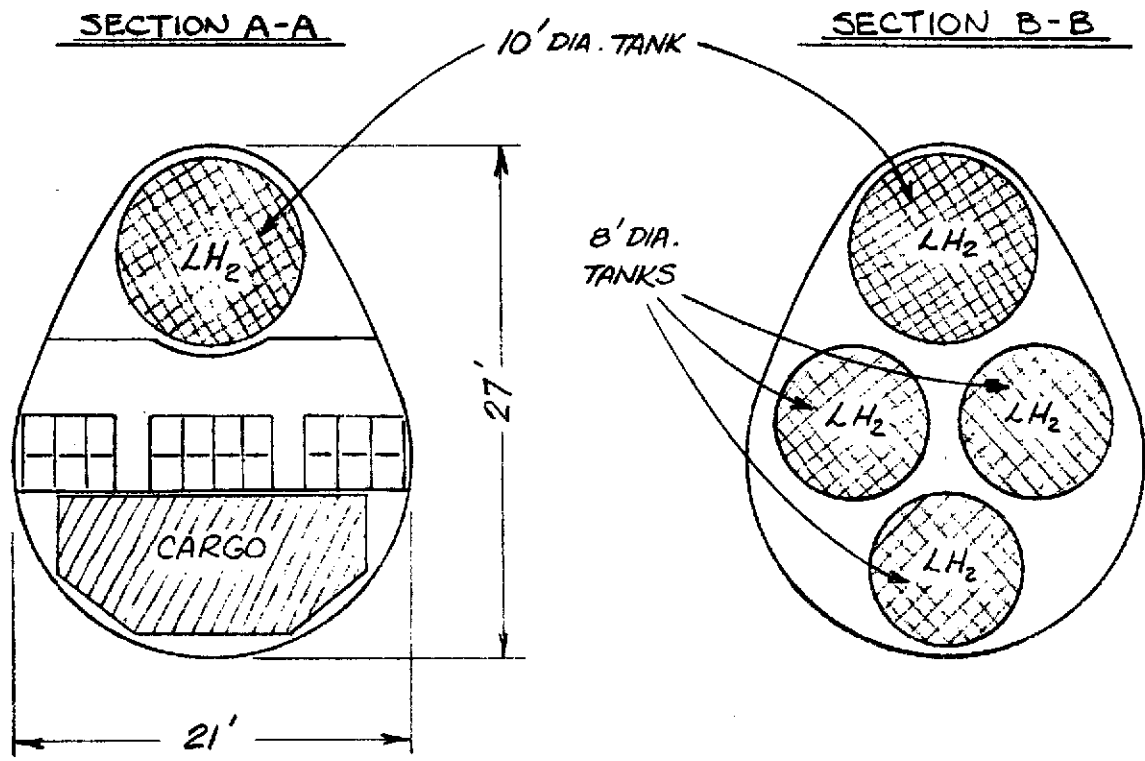
FIGURE 4. — FUSELAGE CROSS-SECTIONS OF 450-PASSENGER LH$_2$ AIRPLANE (SEE PREVIOUS FIGURE).

WING WEIGHT →

$f_{\bar{w}}$ →
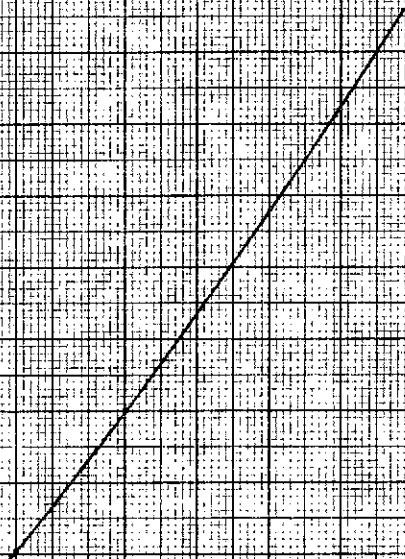
$$f_w = \frac{(WN)^a \, (S \, AR)^b}{\cos \Lambda_{c/4}} \left[\frac{(1 - \frac{W_z}{W})(1 + \lambda)}{(t/c)} \right]^c K$$

$W = $ MAX. FLIGHT GROSS WEIGHT, LB

$N = $ ULTIMATE LOAD FACTOR

$S = $ WING AREA, FT^2

$\Lambda_{c/4} = $ WING SWEEPBACK ANGLE @ QUARTER CHORD

$W_z = (W_{POWERPLANT} + W_{FUEL})$ IN WING, LB

$\lambda = $ TAPER RATIO, TIP CHORD / ROOT CHORD

$t/c = $ THICKNESS / CHORD @ SIDE OF BODY, %

$a, b, c, K = $ CONSTANTS

FIGURE 6. — WING WEIGHT
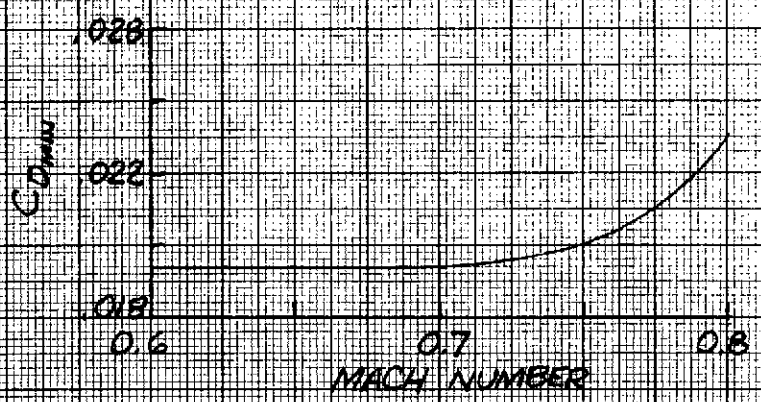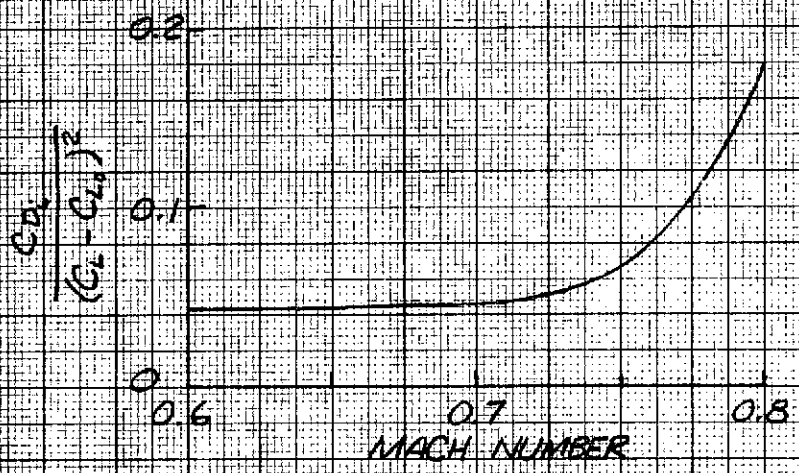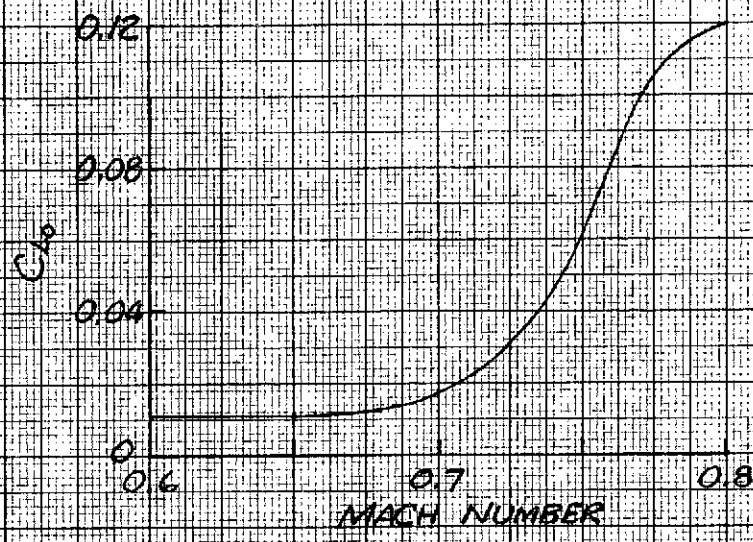
FIGURE 6. — AERODYNAMICS FOR 100 PASS. 900 N.MI. RANGE AIRPLANE
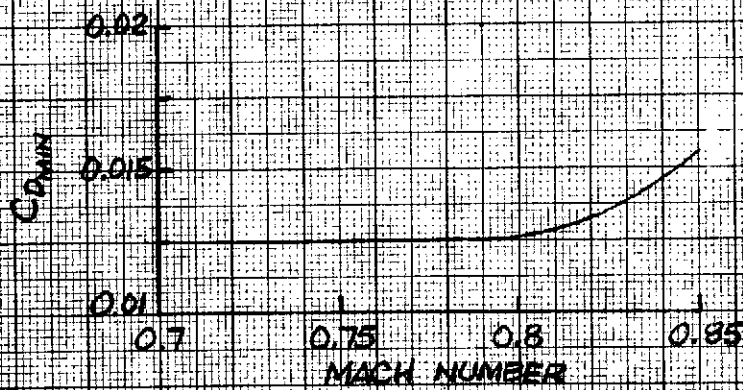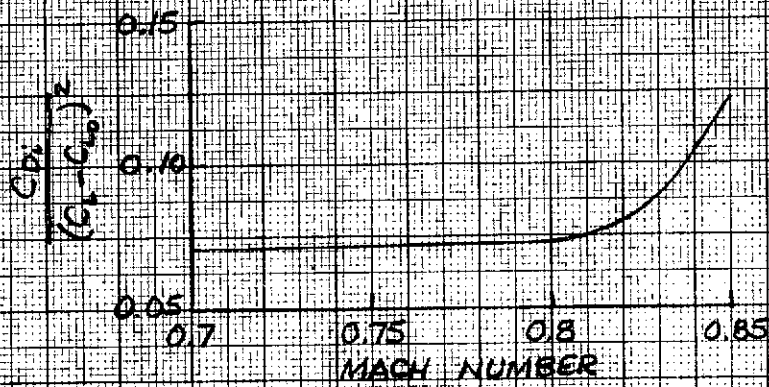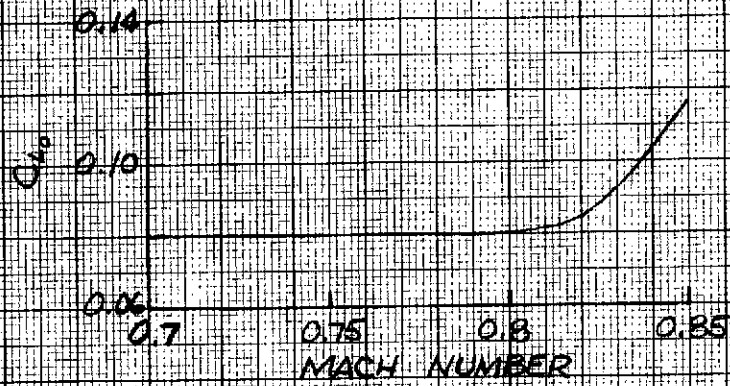
FIGURE 7. — AERODYNAMICS FOR 450 PASS, 3500 N.MI. RANGE AIRPLANE.
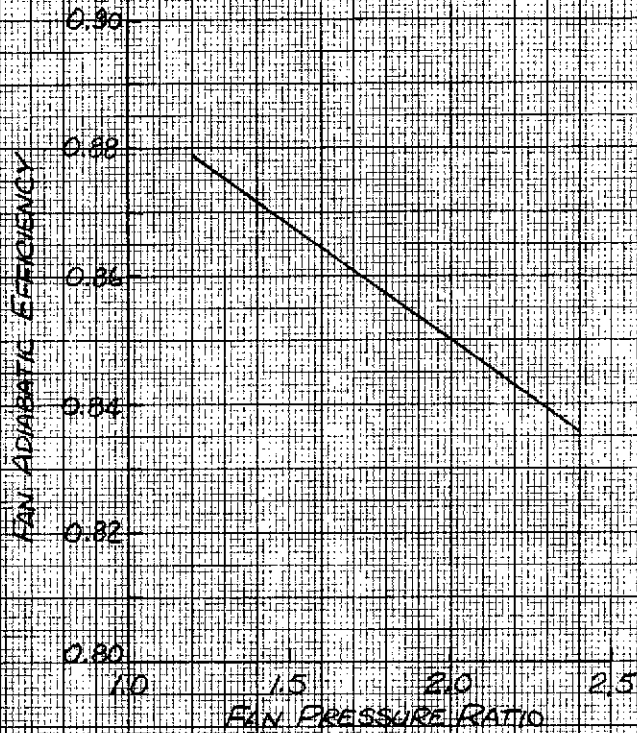
FIGURE 8 — FAN DESIGN EFFICIENCY

Fan Adiabatic Efficiency (vertical axis): 0.80, 0.82, 0.84, 0.86, 0.88, 0.90

Fan Pressure Ratio (horizontal axis): 1.0, 1.5, 2.0, 2.5
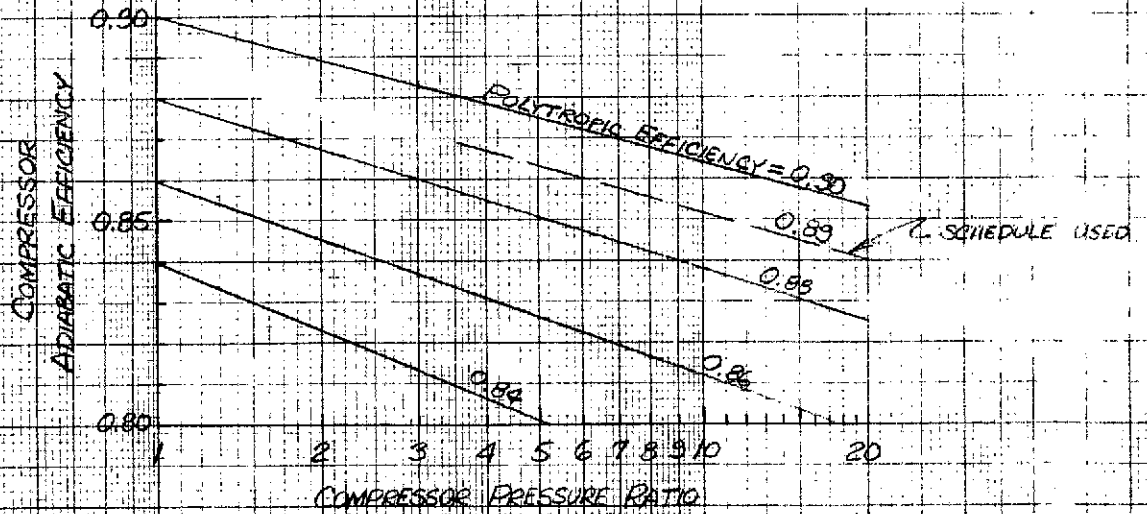
FIGURE 9 — COMPRESSOR DESIGN EFFICIENCY

Compressor Adiabatic Efficiency (vertical axis): 0.80, 0.85, 0.90

Compressor Pressure Ratio (horizontal axis): 1, 2, 3, 4, 5, 6, 7, 8, 9, 10, 20

POLYTROPIC EFFICIENCY = 0.90

0.89

0.88

0.86

% SCHEDULE USED
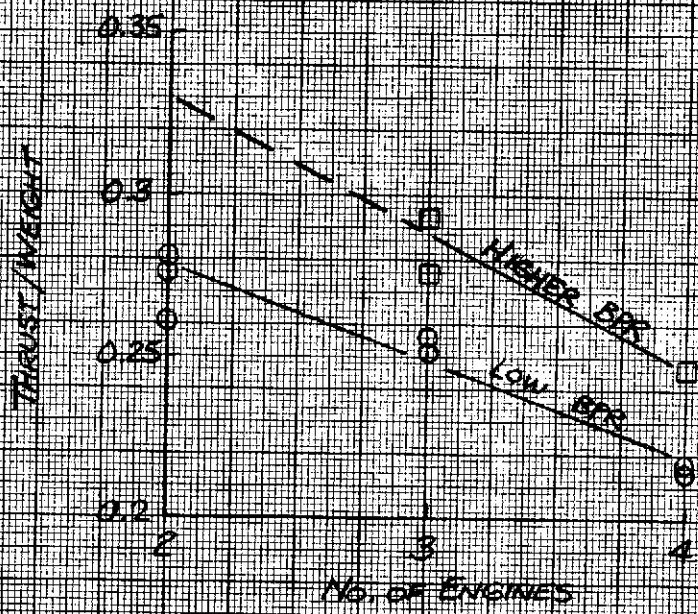
FIGURE 10. — TAKEOFF THRUST/WEIGHT FOR CURRENT COMMERCIAL TRANSPORTS
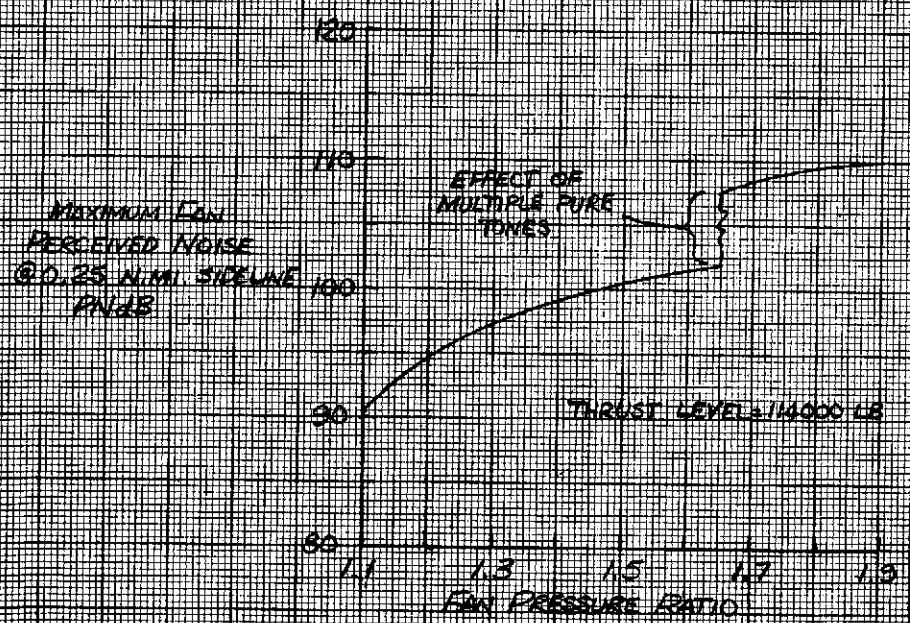
FIGURE 11. — FAN MACHINERY NOISE
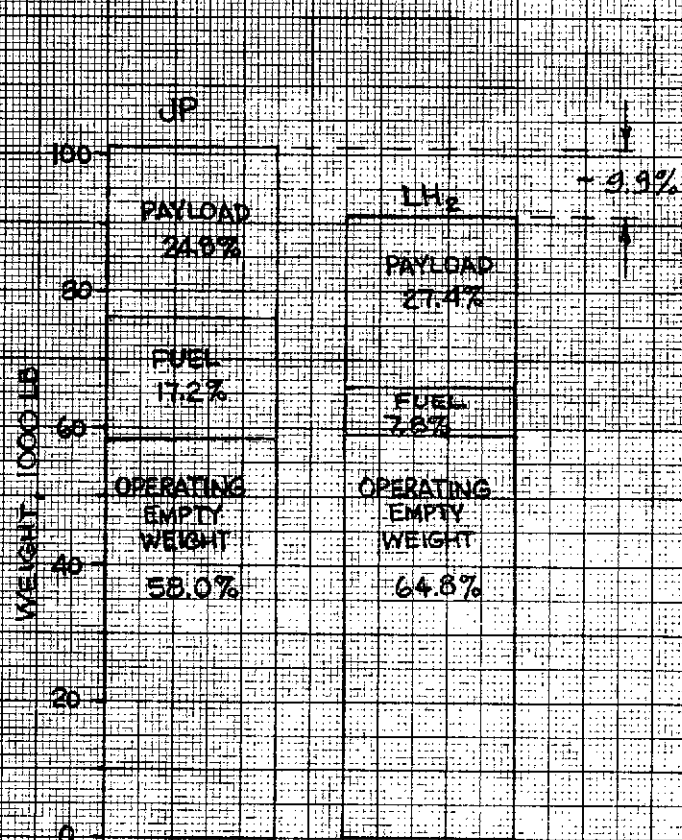
FIGURE 12. — REPRESENTATIVE WEIGHT BREAKDOWNS
FOR JP AND LH₂ FUELED AIRPLANES.
(FPR = 1.5, OPR = 28, BPR = 8.8)
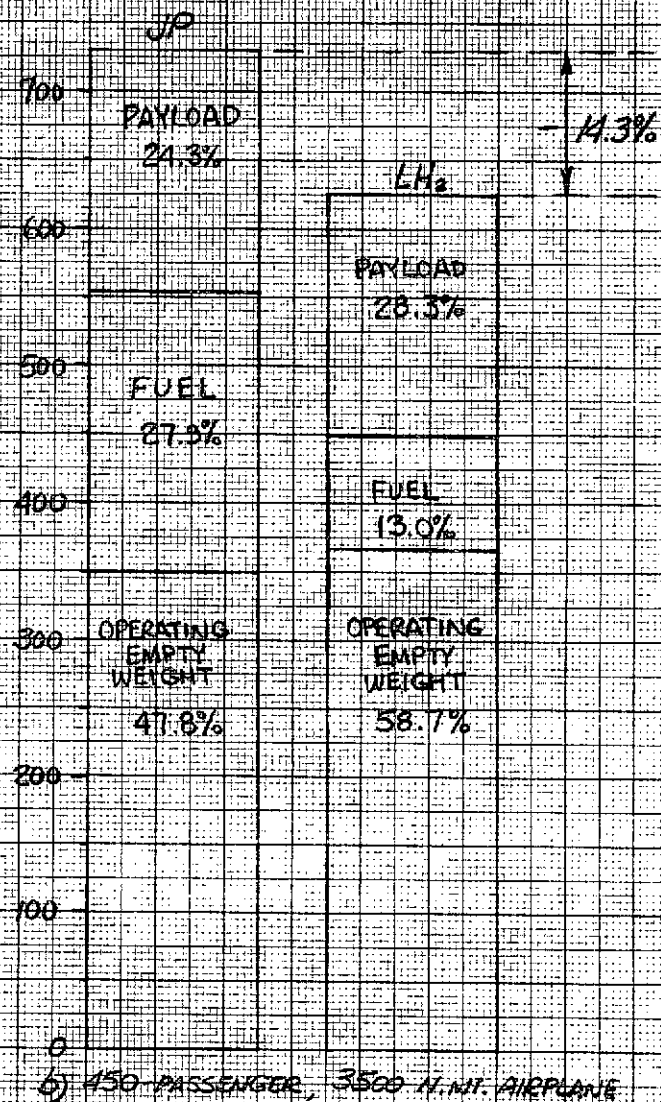
a) 100-PASSENGER, 900 N.MI. AIRPLANE

b) 450-PASSENGER, 3500 N.MI. AIRPLANE
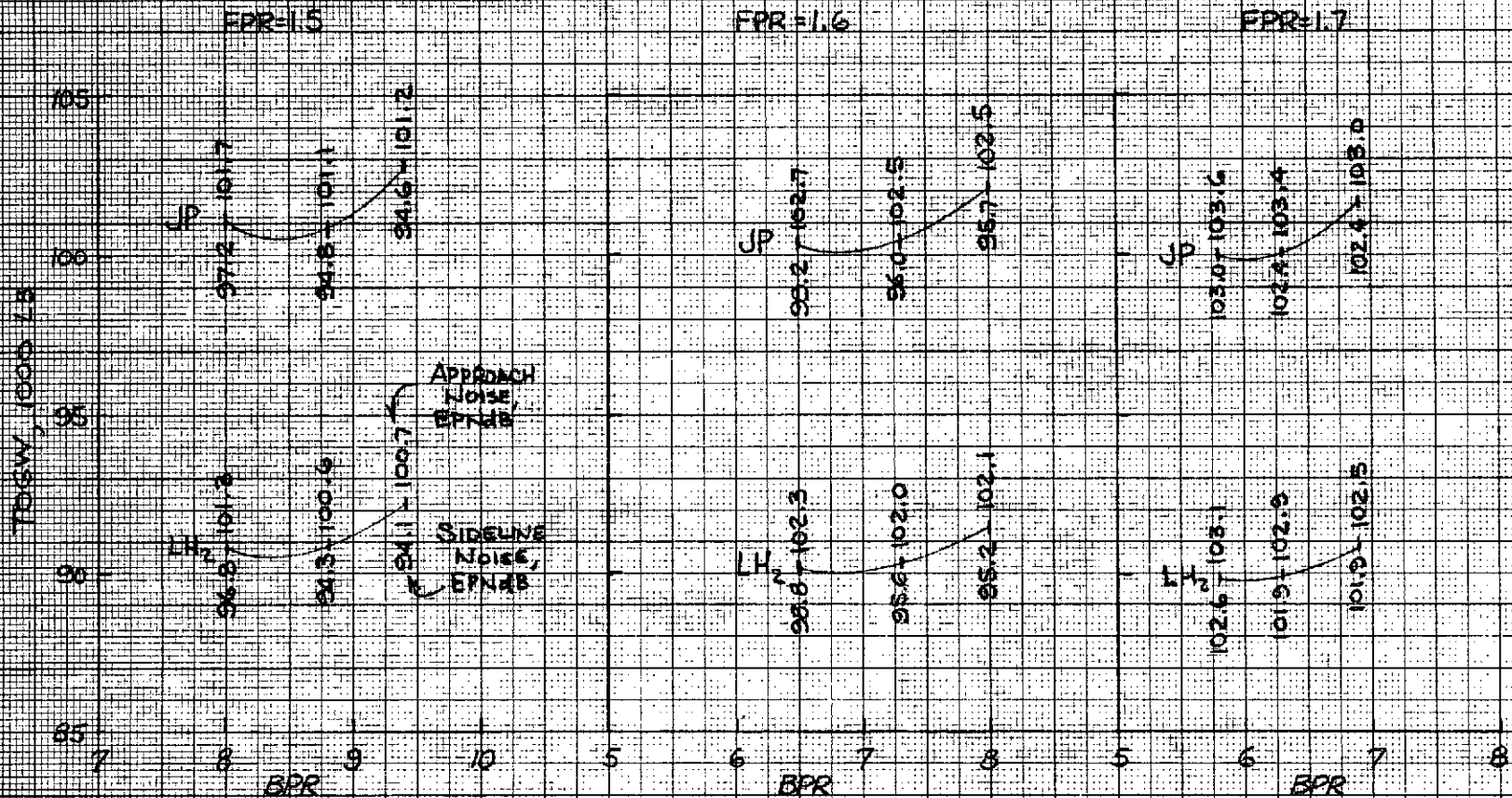
FIGURE 13 -- TAKEOFF GROSS WEIGHT VARIATION WITH FPR AND BPR FOR 100-PASSENGER AIRPLANE.
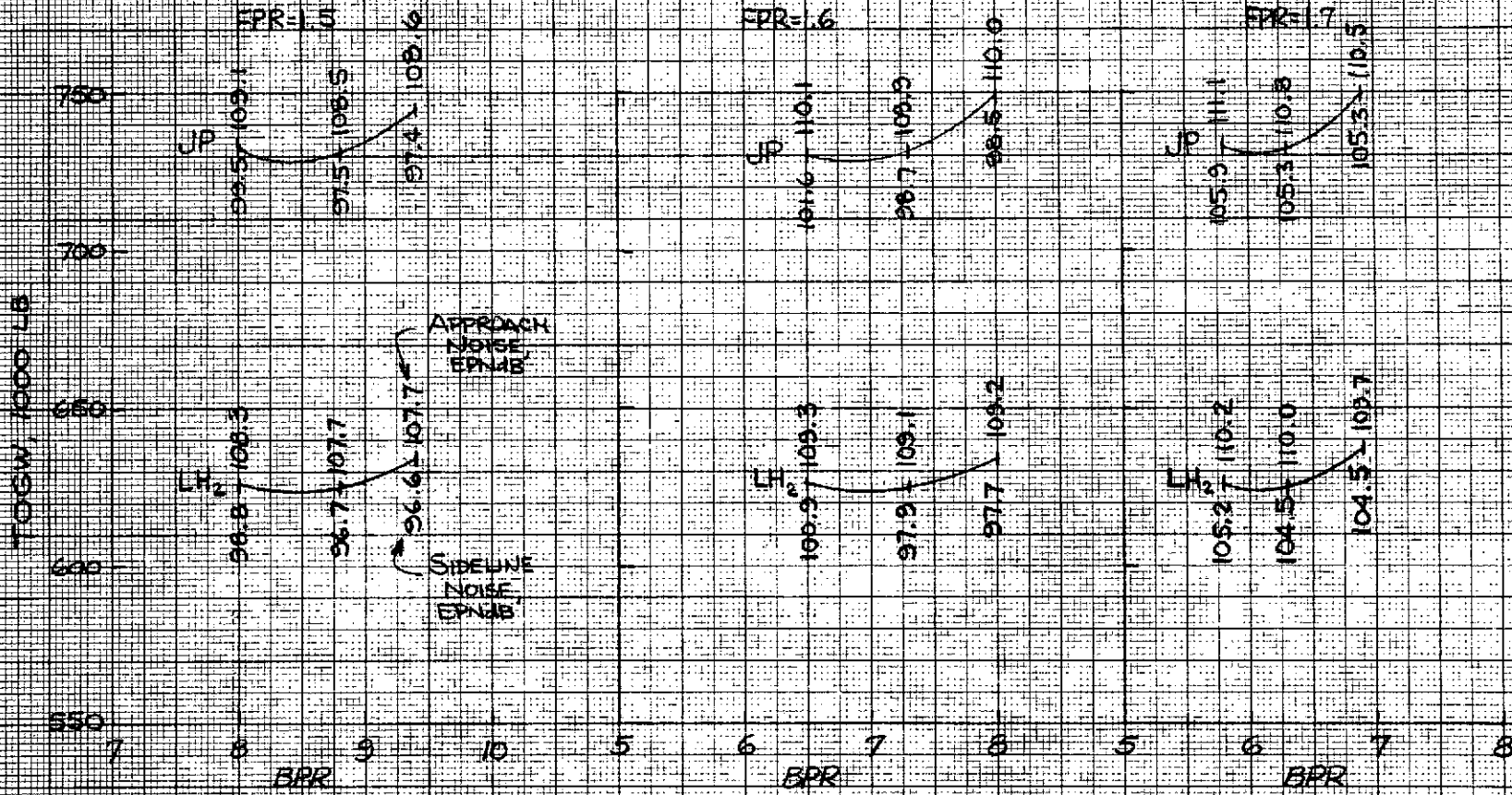
FIGURE 14 - TAKEOFF GROSS WEIGHT VARIATION WITH FPR AND BPR FOR 450-PASSENGER AIRPLANE
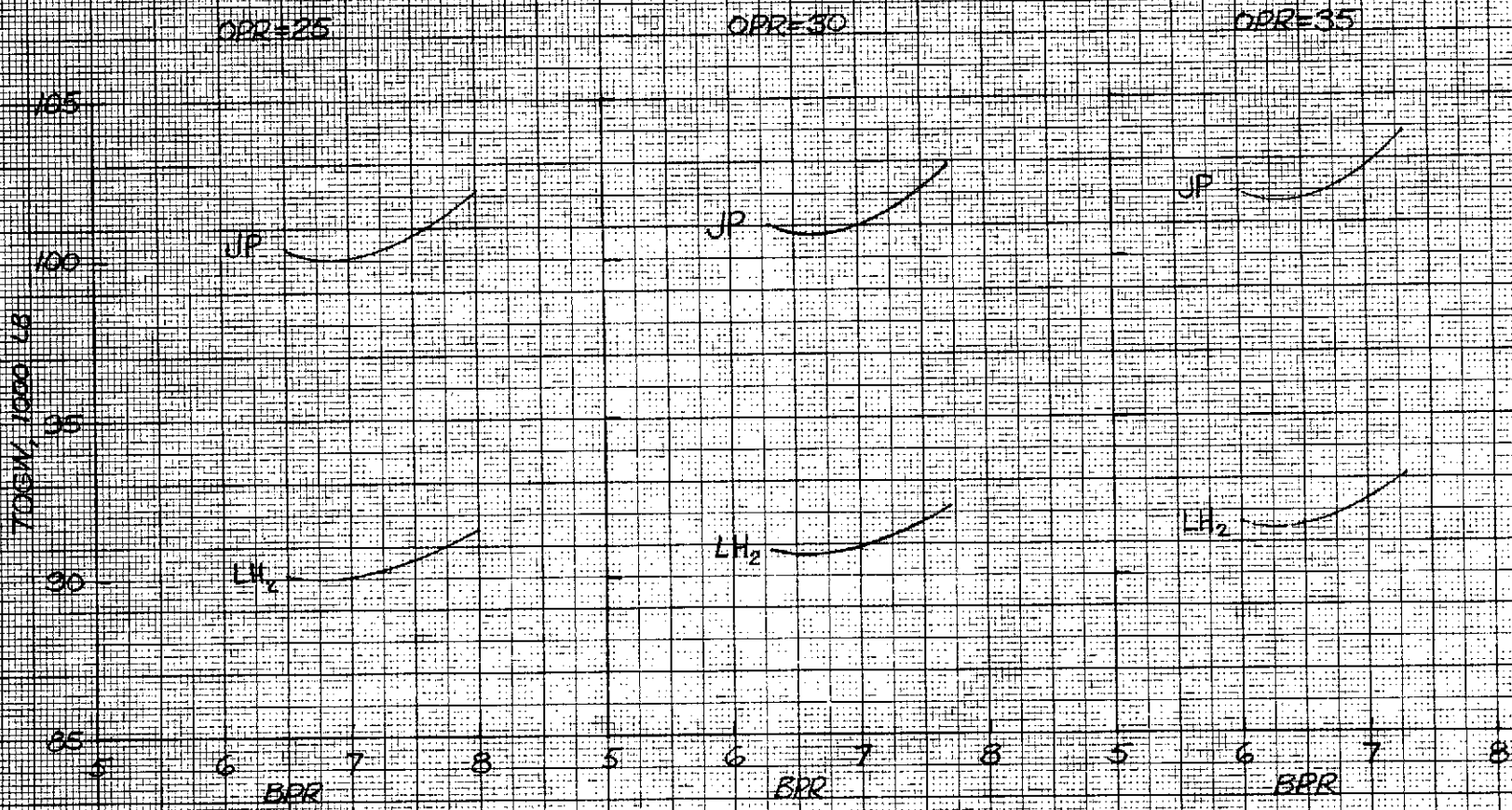
FIGURE 15 — TAKEOFF GROSS WEIGHT VARIATION WITH OPR FOR 100-PASSENGER AIRPLANE.
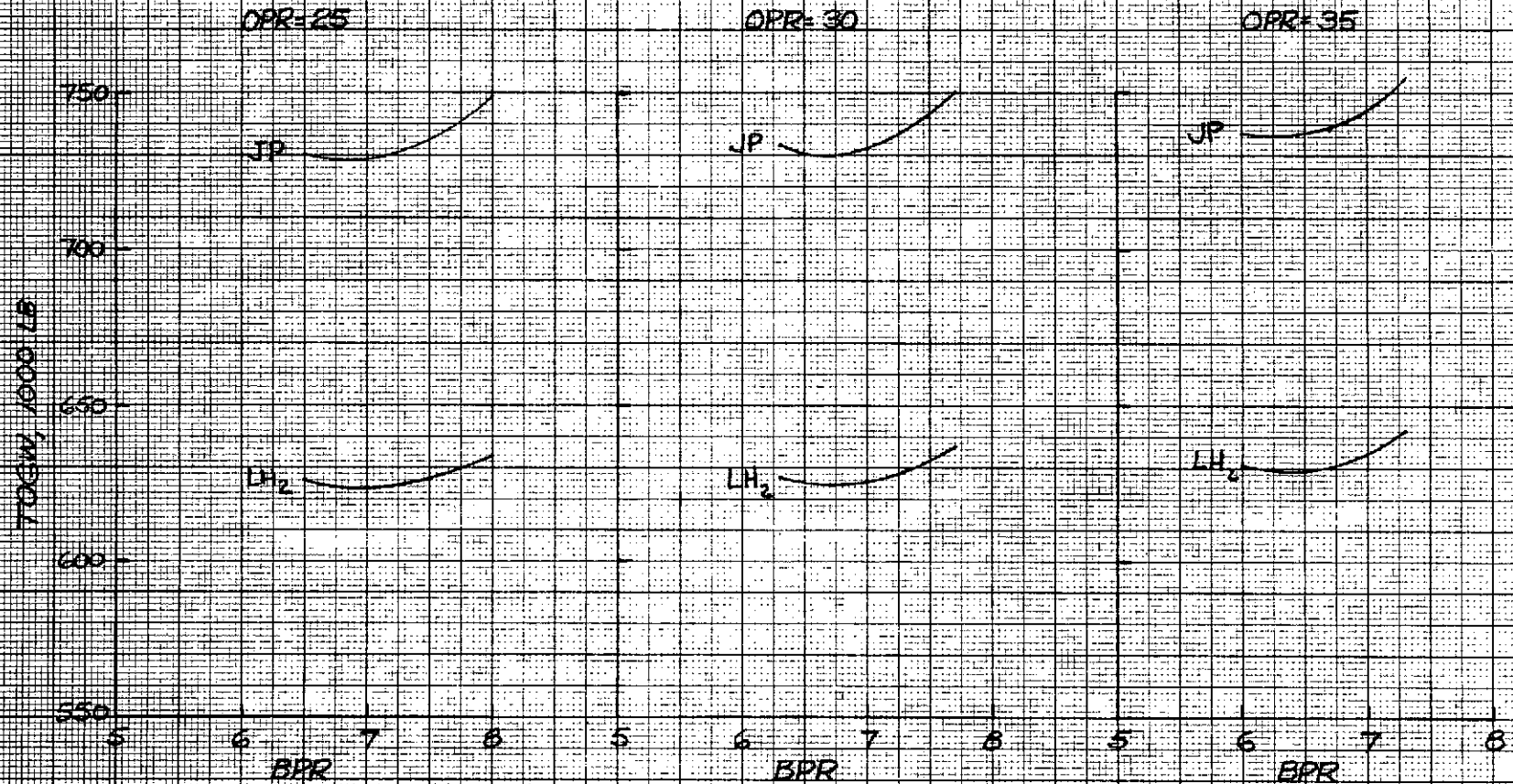
FIGURE 16 — TAKEOFF GROSS WEIGHT VARIATION WITH OPR FOR 450-PASSENGER AIRPLANE.
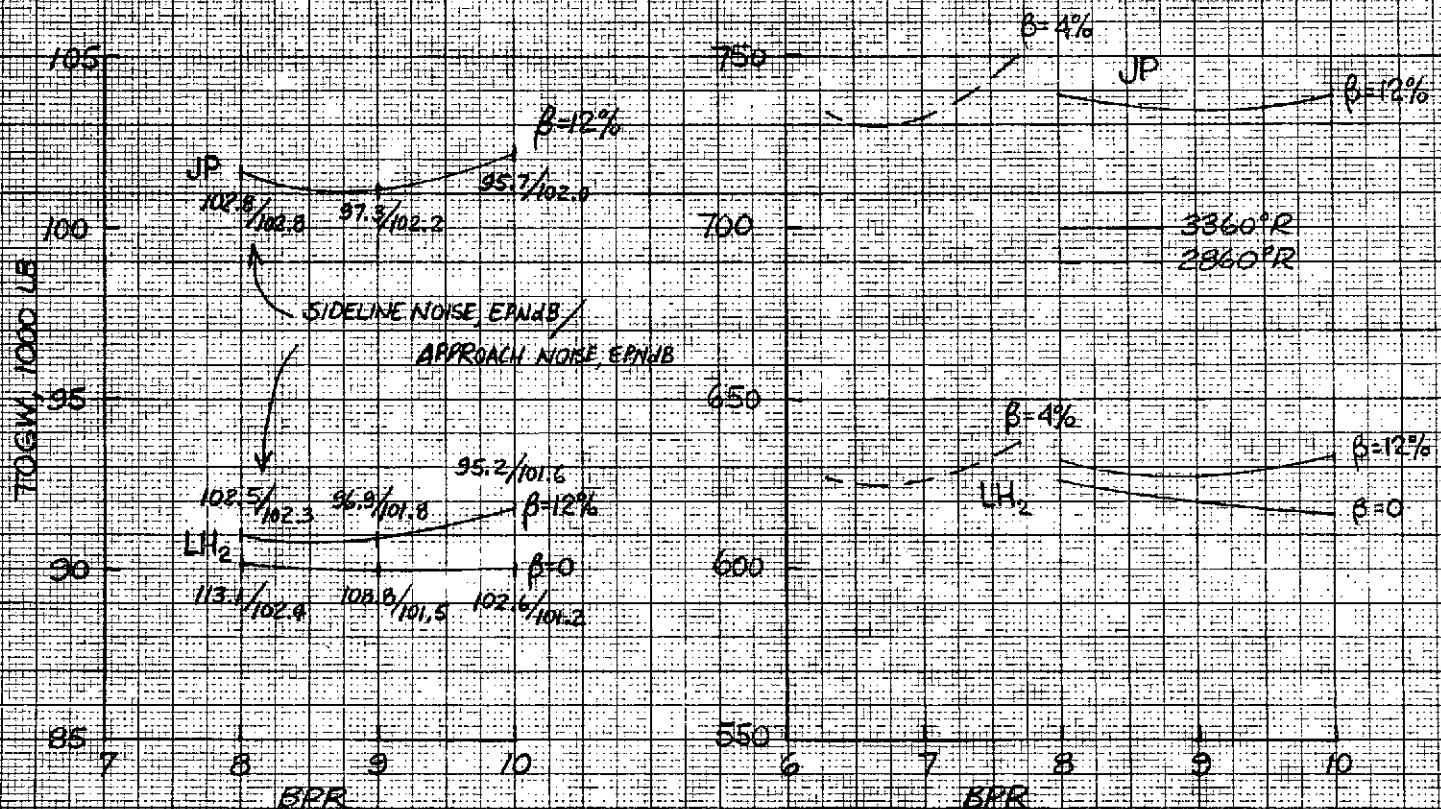
FIGURE 17. — EFFECT OF HIGHER T_4 AND ELIMINATION OF COOLING BLEED AIR FOR LH_2 AIRPLANE
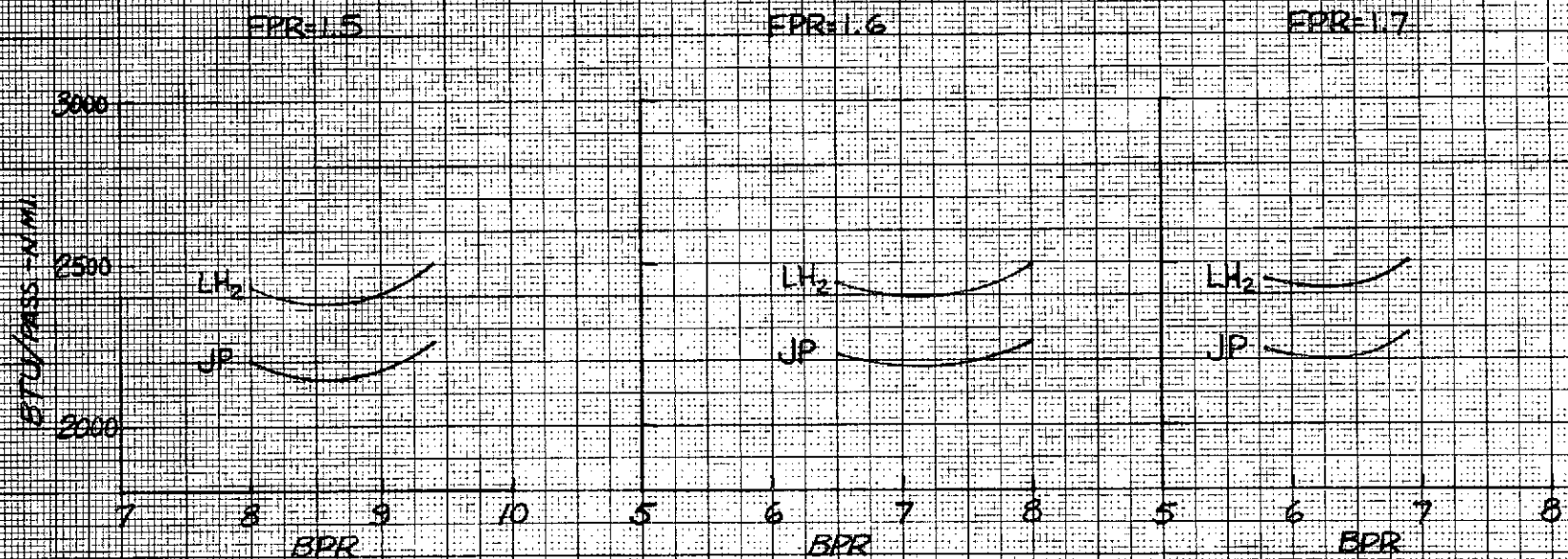
FIGURE 18.— ENERGY CONSUMPTION FOR 100-PASS AIRPLANE
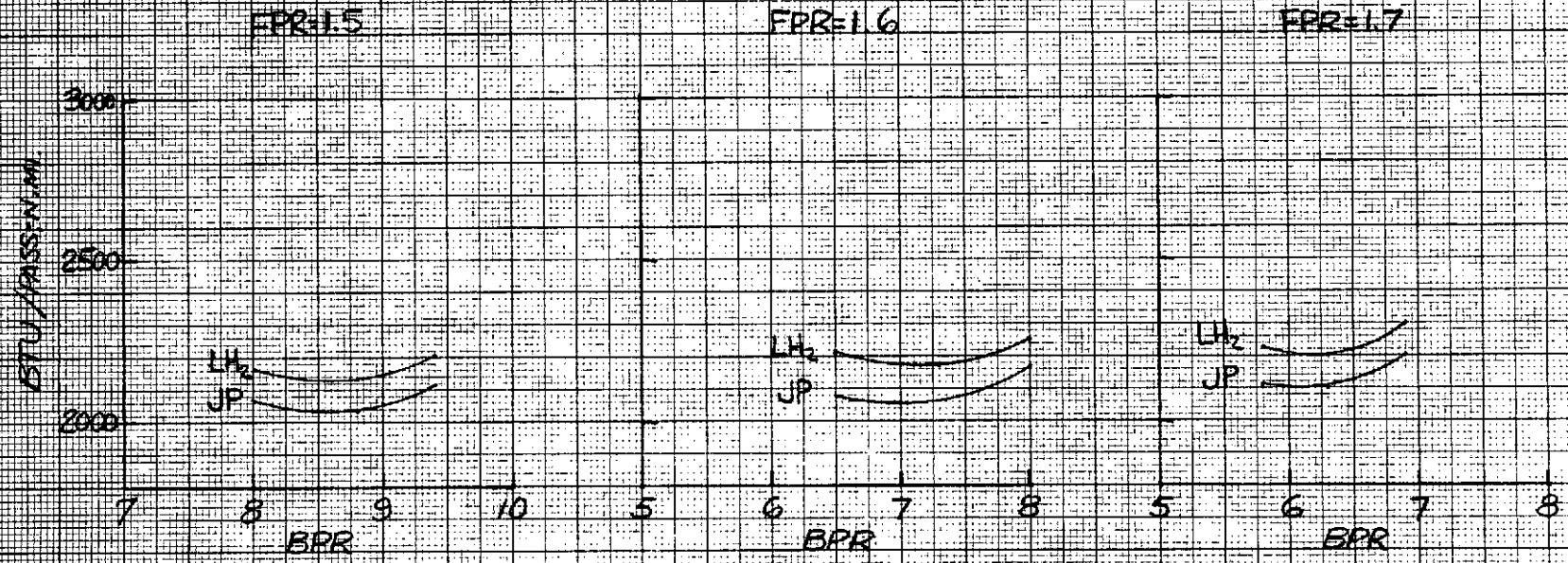
FIGURE 19. — ENERGY CONSUMPTION FOR 450-PASS. AIRPLANE
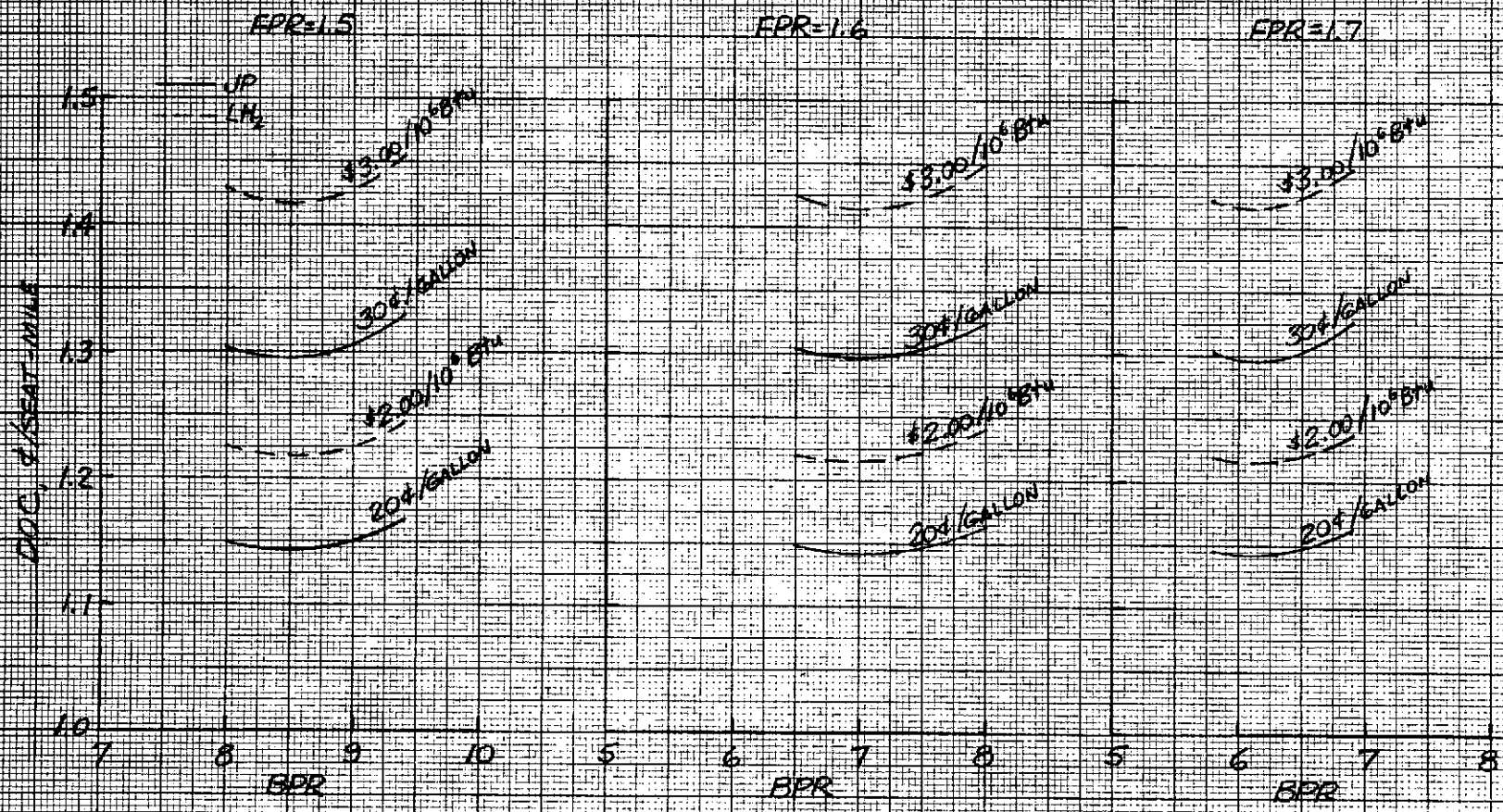
FIGURE 20 — DOC VARIATION WITH FAN PRESSURE RATIO AND BYPASS RATIO FOR 100-PASSENGER AIRPLANE
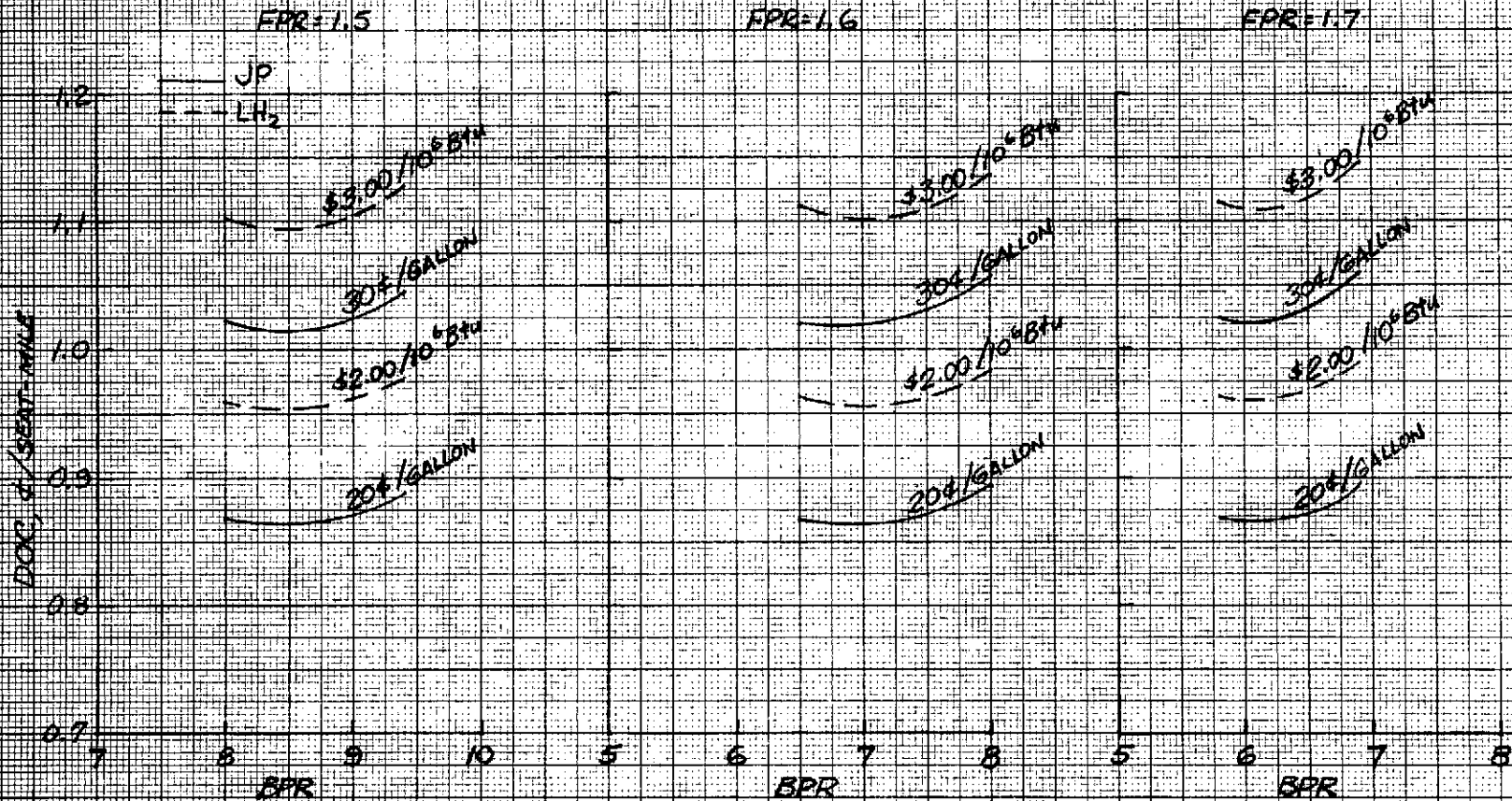
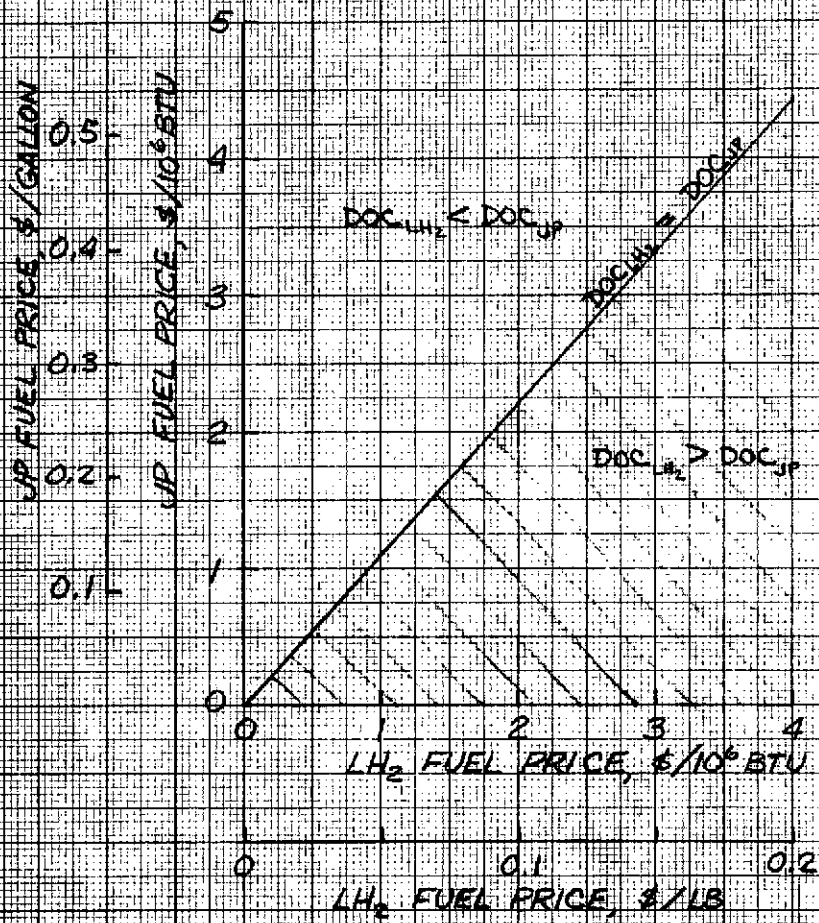FIGURE 21. — DOC VARIATION WITH FAN PRESSURE RATIO AND BYPASS RATIO FOR 450-PASSENGER AIRPLANE

FIGURE 22. — BREAK-EVEN PRICES OF JP AND LH₂ FUEL. (BASED ON FPR=1.5, OPR=25, BPR=8.8, T₄=2860°R, 100-PASS AIRPLANE)
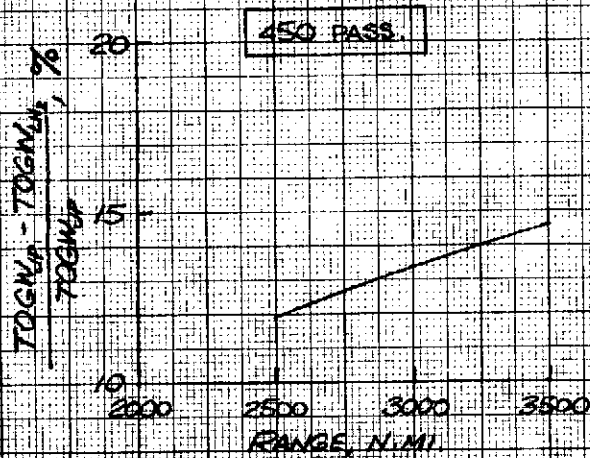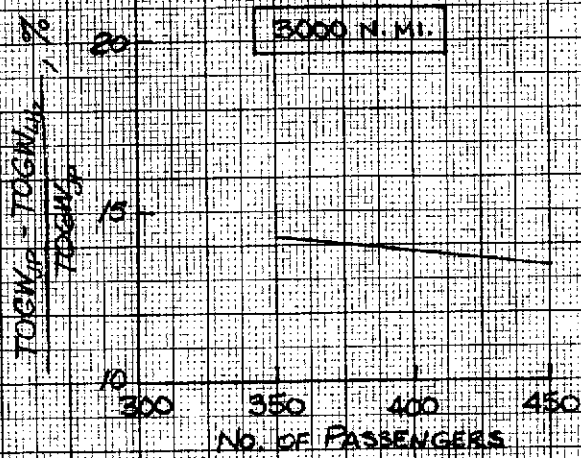
FPR=1.6, OPR=25, BPR=7.3

3000 N. MI.

$\dfrac{TOGW_{JP} - TOGW_{LH_2}}{TOGW_{JP}}$, %

No. of Passengers

450 PASS.

$\dfrac{TOGW_{JP} - TOGW_{LH_2}}{TOGW_{JP}}$, %

Range, N.MI.

FIGURE 23.— SENSITIVITY OF LH₂ GROSS WEIGHT
IMPROVEMENT WITH DESIGN RANGE
AND PAYLOAD